Graphite Properties and Characteristics

For industrial applications

Entegris
POCO Materials

INTRODUCTION

Entegris' POCO Materials are routinely used in a wide range of highly technical industrial applications. As we continue to grow our market share of manufactured graphite material and expand their usage into increasingly complex areas, the need for the market to be more technically versed in graphite properties and how they are tested has also grown. It is with this thought in mind that we developed this primer on graphite properties and characteristics.

We have been a graphite supplier to industrial industries for more than 50 years. Products include APCVD wafer carriers, E-Beam crucibles, heaters (small and large), ion implanter parts, LTO injector tubes, MOCVD susceptors, PECVD wafer trays and disk boats, plasma etch electrodes, quartz replacement parts, sealing plates, bonding fixtures, and sputtering targets. Our wide range of materials, as well as post-processing and machining capabilities, continuously meet the demanding requirements of semiconductor processing.

We have accumulated experience from over 50 years of testing graphite grades across the industry. With this expertise, we can describe the relationship between graphite material properties and explain their testing methods. These properties also highlight why our materials are industry leading.

The purpose of this document is to introduce the reader to graphite properties and to describe testing techniques that enable true comparisons between a multitude of manufactured graphites. Our graphites come in many grades, each designed for a specific range of applications. In the semiconductor industry, grades include ZXF-5Q, ACF-10Q, AXF-5Q, AXF-5QC, AXZ-5Q, AXM-5Q and HPD. These are the materials upon which we have built our reputation as a leading manufacturer of the world's best graphites.

TABLE OF CONTENTS

STRUCTURE

DEFINITION: CARBON, THE ELEMENT

Carbon is the sixth element on the periodic table and can be found in abundance in the sun, stars, comets, and atmospheres of most planets.

Carbon is a Group 14 element (on older periodic tables, Group IVA) along with silicon, germanium, tin, and lead. Carbon is distributed very widely in nature, Figure 1-1.
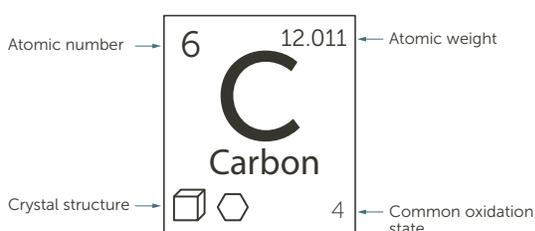

Figure 1-1. Carbon as depicted on the periodic table

In 1961, the International Union of Pure and Applied Chemistry (IUPAC) adopted the isotope ^{12}C as the basis for atomic weights. Carbon-14, ^{14}C, an isotope with a half-life of 5730 years, is used to date such materials as wood, archeological specimens, etc. Carbon-13, ^{13}C, is particularly useful for isotopic labeling studies since it is not radioactive, but has a spin I = ½ nucleus and therefore a good NMR nucleus.

Carbon has four electrons in its valence shell (outer shell). The electron configuration in carbon is $1s^2\ 2s^2\ 2p^2$. Since this energy shell can hold eight electrons, each carbon atom can share electrons with up to four different atoms. This electronic configuration gives carbon its unique set of properties (Table 1-1). Carbon can combine with other elements as well as with itself. This allows carbon to form many different compounds of varying size and shape.

Carbon is present as carbon dioxide in the atmosphere and dissolved in all natural waters. It is a component of rocks as carbonates of calcium (limestone), magnesium, and iron. Coal, petroleum, and natural gas are chiefly hydrocarbons. Carbon is unique among the elements in the vast number of varieties of compounds it can form. Organic chemistry is the study of carbon and its compounds.

Table 1-1. Properties of the element carbon

Name	Carbon
Symbol	C
Atomic number	6
Atomic mass	12.0107 amu
Melting point	3500.0°C 3773.15 K 6332.0°F
Boiling point	4827.0°C 5100.15 K 8720.6°F
Number of protons/electrons	6
Number of neutrons	6, 7, 8
Classification	Nonmetal
Crystal structure	Hexagonal Cubic
Density @ 293 K	Graphite – 2.26 g/cm³ Diamond – 3.53 g/cm³
Color	Black, gray

The history of manufactured graphite began at the end of the 19th century with a surge in carbon manufacturing technologies. The use of the electrical resistance furnace to manufacture synthetic graphite led to the development of manufactured forms of carbon in the early part of the 20th century and more recently, to a wide variety of high-performance materials such as carbon fibers and nanotubes, Figure 1-2.

FORMS OF CARBON

Carbon is found free in nature in three allotropic forms: amorphous carbon, graphite, and diamond. More recently, a fourth form of carbon, buckminsterfullerene, C_{60}, has been discovered. This new form of carbon is the subject of great interest in research laboratories today. Within the past few years, this research has centered on graphene and its derivatives, which have the potential to bring about a fundamental change in the semiconductor/electronic industry.

Carbon alone forms the familiar substances graphite and diamond. Both are made only of carbon atoms. Graphite is very soft and slippery, while diamond is one of the hardest substances known to man. Carbon, as microscopic diamonds, is found in some meteorites. Natural diamonds are found in ancient volcanic "pipes" like those found in South Africa. If both graphite and diamond are made only of carbon atoms, what gives them different properties? The answer lies in the way the carbon atoms form bonds with each other.

Pre-1880
— Lampblack (writing)
— Charcoals (gunpowder, medicine, deodorants)
— Natural graphite (writing material)

1880–1940
— Activated carbons
— Carbon blacks
— Coal coking (coal-tar pitch)
— Delayed coking
— Synthetic graphite and diamond

1940-2013
— Carbon fibers (PAN)
— Carbon fibers (pitch-based)
— Carbon fibers (microporous)
— Carbon/resin composites
— Carbon/carbon composites
— Specialty activated carbons
— Carbon as a catayst support
— Carbon whiskers/filaments
— Prosthetics
— Intercalation compounds
— Graphite/oxide refractories
— Pyrolytic carbon
— Glassy carbon
— Mesocarbon microbeads
— Diamond films
— Diamond-like films
— Elastic carbon
— Fullerenes
— Nanotubes
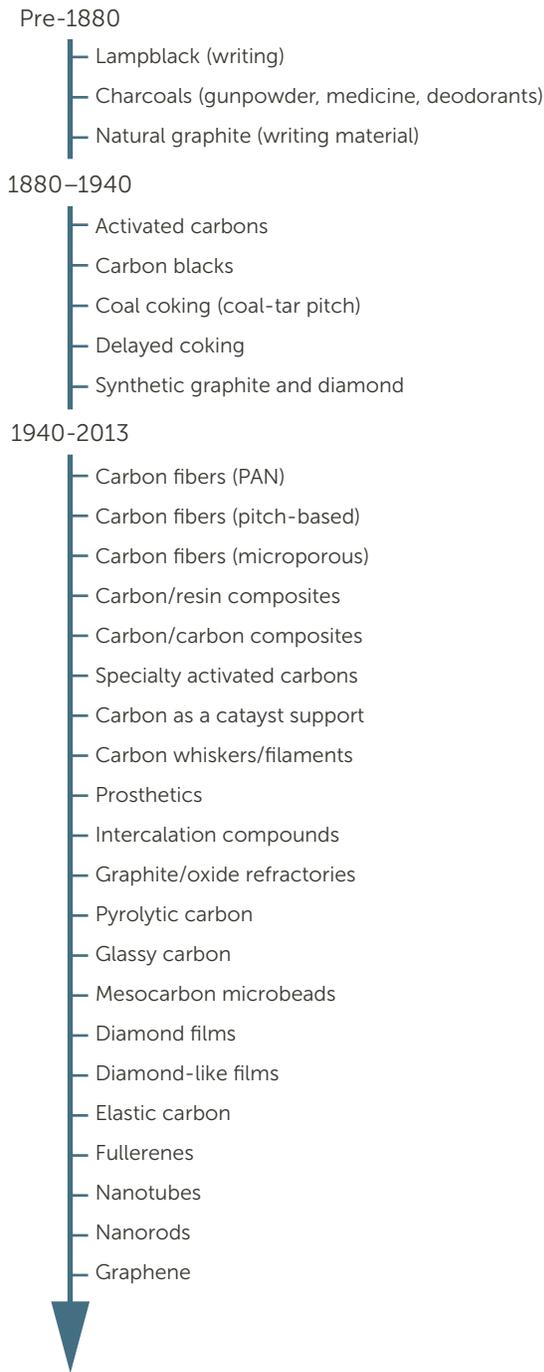— Nanorods
— Graphene

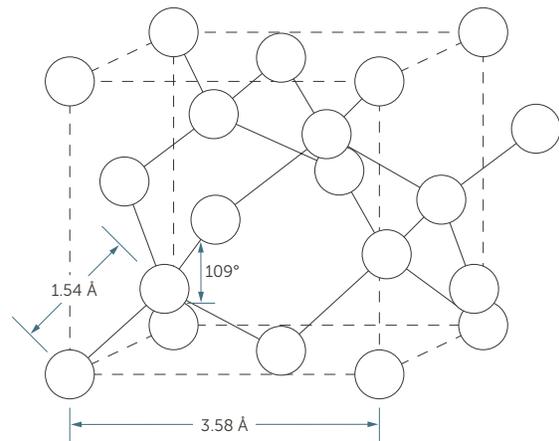Figure 1-2. Growth of carbon materials[1]

Figure 1-3. The crystal structure of diamond

The forces within and between crystallites determine the extreme difference in properties between these two forms. In diamond, the crystal structure is face-centered cubic, Figure 1-3. The interatomic distance is 1.54 Å with each atom covalently bonded to four other carbons in the form of a tetrahedron. This interatomic distance is close to that found in aliphatic hydrocarbons, which is in distinction to the smaller 1.42 Å carbon-carbon distance found in graphite and aromatic hydrocarbons (1.39 Å in benzene). This three-dimensional isotropic structure accounts for the extreme hardness of diamond.
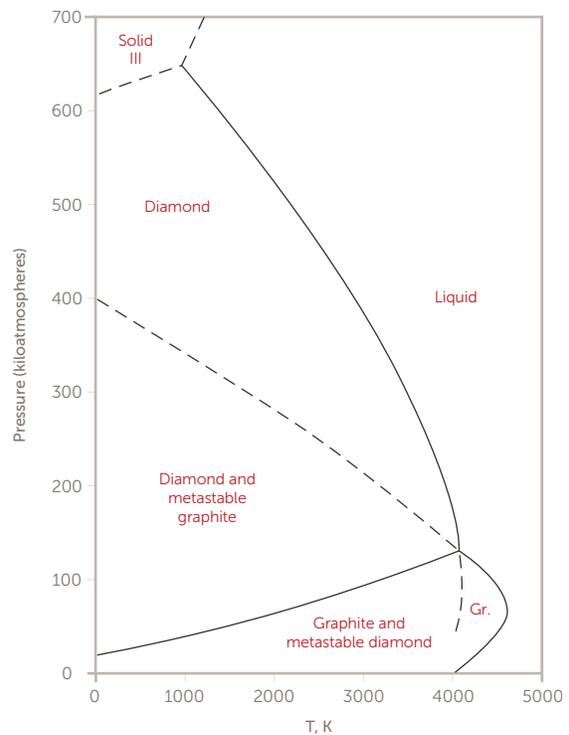

Figure 1-4. The carbon phase diagram

Thermodynamically, graphite at atmospheric pressure is the more stable form of carbon. Diamond is transformed to graphite above 1500°C (2732°F), Figure 1-4.
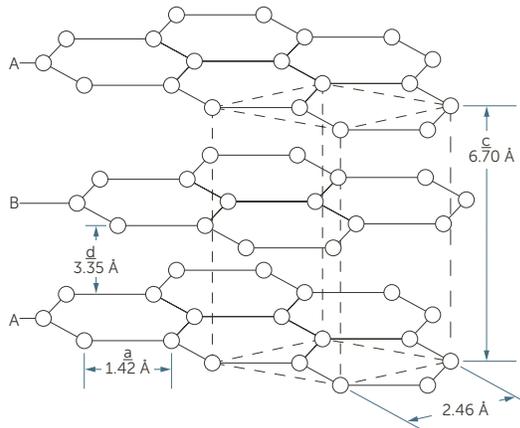

Figure 1-5. The crystal structure of graphite

The structure of graphite consists of a succession of layers parallel to the basal plane of hexagonally linked carbon atoms. The ideal graphite structure is shown in Figure 1-5.

In this stable hexagonal lattice, the interatomic distance within a layer plane, a, is 1.42 Å and the interlayer distance, d, between planes is 3.35 Å. Crystal density is 2.266 g/cm³ as compared with 3.53 g/cm³ for diamond. In the graphite structure (sp² hybridization), only three of the four valence electrons of carbon form regular covalent bonds (σ-bonds) with adjacent carbon atoms. The fourth or π electron resonates between the valence bond structures. Strong chemical bonding forces exist within the layer planes, yet the bonding energy between planes is only about two percent of that within the planes (150 – 170 kcal/[gram atom] vs. 1.3 – 4 kcal/[gram atom]). These weaker bonds between the planes are most often explained to be the result of van der Waals forces.

However, Spain[2] identifies the π orbital, which has a p_z configuration, and not van der Waals forces as the correct source of bonding between the adjacent layers. In general, the π bands overlap by ~40 meV to form the three-dimensional graphite network where the layer planes are stacked in the ABAB sequence illustrated in Figure 1-5. Spain concludes in his discussions on electronic structure and transport properties of graphite that the overlap of π orbitals on adjacent atoms in a given plane also provides the electron bond network responsible for the high mobility (electronic) of graphite.

This would appear more correct, since van der Waals forces are the result of dipole moments, which would not account for the high mobility.

Consequently, weak forces between layer planes account for, (a) the tendency of graphitic materials to fracture along planes, (b) the formation of interstitial compounds, and (c) the lubricating, compressive, and many other properties of graphite.

As previously mentioned for the hexagonal graphite structure, the stacking order of planes is ABAB, so that the atoms in alternate planes are congruent, Figure 1-5. Studies have shown that natural graphite contains 17 to 22 percent of a rhombohedral structure with a stacking sequence of ABCABC. In "artificial" or "synthetic" graphite, in the as-formed state, only a few percent at best could be found. However, deformation processes such as grinding substantially increase the percent of rhombohedral structure found in the otherwise hexagonal structure.

Amorphous carbon is also referred to as nongraphitic carbon. When examined by X-ray diffraction, these materials show only diffuse maxima at the normal scattering angles. This has been attributed to a random translation and rotation of the layers within the layer planes. This disorder has been called turbostratic. Some of these nongraphitic carbons will become graphitic, upon heating to 1700° – 3000°C (3092° – 5432°F). Some will remain nongraphitic above 3000°C (5432°F).

Thus far, the discussion has centered on the crystal structure of graphites. On a more macroscopic level, the structure as routinely examined on a light microscope at magnifications of 100, 200, and 500 times reveals the porosity, particle or grain size, and the general microstructure as it is commonly referred to. Photomicrographs of AXF-5Q graphite compared to a conventional graphite demonstrate some significant differences when viewed at 100× magnification, Figure 1-6, and at 500× magnification, Figure 1-7. It can be seen from these photos that vast differences do exist in graphite microstructure. These differences are directly related to raw material and processing parameters.

As seen in the photos, the dark or black regions represent the porosity while the lighter regions represent the graphite matrix. It is this matrix, composed of smaller particles bound together either chemically or mechanically, that comprises crystals stacked layer upon layer. This is more easily seen in scanning electron micrographs (SEM).
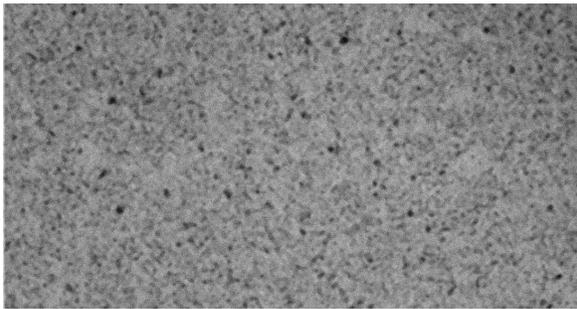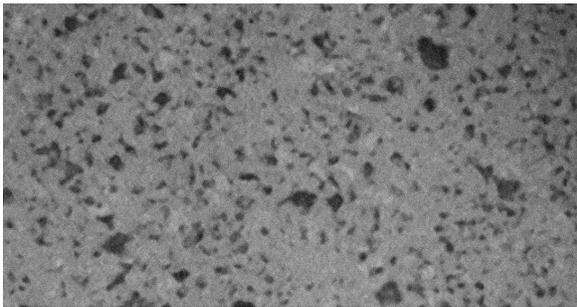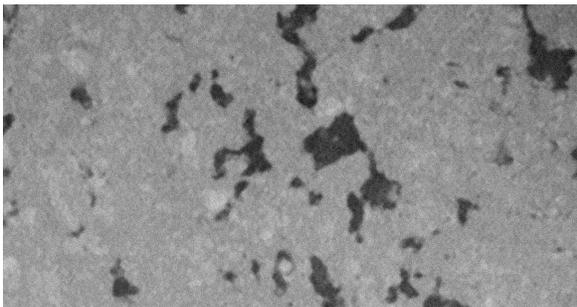
AXF-5Q Graphite — 100× magnification
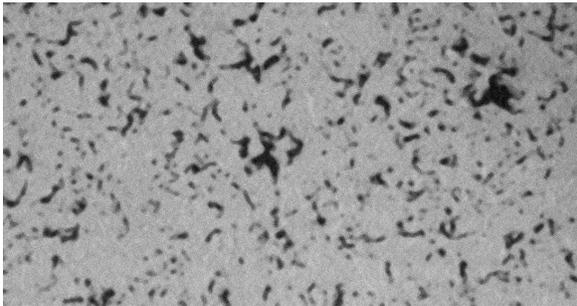
Conventional Graphite — 100× magnification

Figure 1-6. AXF-5Q graphite vs. conventional graphite under light microscope at 100× magnification

AXF-5Q Graphite — 500× magnification

Conventional Graphite — 500× magnification

Figure 1-7. AXF-5Q graphite vs. conventional graphite under light microscope at 500× magnification
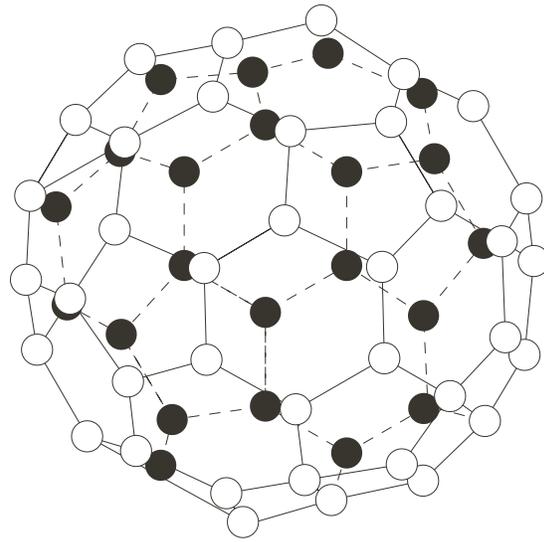

Figure 1-8. The crystal structure of C_{60} , fullerene

The fourth form of carbon, buckminsterfullerene, formula C_{60}, whose framework is reminiscent of the seams in an association football ("soccer") ball, Figure 1-8, is the subject of considerable interest at present and was only discovered a few years ago in work involving Harry Kroto, a Sheffield University graduate.

TEST METHODS

The structure of graphite has been determined through such methods as X-ray diffraction, transmission electron microscopy, neutron diffraction, and convergent beam electron diffraction. These methods are highly sophisticated and generally require very expensive equipment with a highly skilled operator. This is normally beyond the scope of typical industrial laboratories. Since this type of testing or analysis is more research-oriented, no standard methods will be presented.

However, several books have been published on the structure of graphite and the reader is encouraged to review the bibliography in the appendix.

STRUCTURAL COMPARISON TO CONVENTIONAL GRAPHITES

With regard to crystalline structure, our graphite has a typical hexagonal structure. The layer spacings may vary, as they are a function of raw material and process conditions and vary from manufacturer to manufacturer. It is reasonable to assume that a certain degree of rhombohedral structure exists also in machined artifacts due to the machining-induced deformation mentioned previously. No testing has been done to confirm this.

Our graphites are also highly isotropic with respect to their structure and properties. The isotropy factor is between 0.97 and 1.03 with 1.00 being perfect. A factor of 1.00 means the properties are identical no matter which direction they are measured. Many conventional graphites are anisotropic. This means the properties vary depending on which direction you test them. The high degree of isotropy makes our graphites useful in many applications where an anisotropic material would fail. It also allows for maximum utilization of material, as machining orientation is of no importance.

TEMPERATURE EFFECTS

There are two general types of carbon, those considered to be "graphitizing" carbons and those that are "non-graphitizing." The most significant differences are found in the apparent layer size and apparent stack height. For equal layer sizes, the apparent stack height, i.e., average number of layers per stack, is less for nongraphitizing carbons than graphitizing carbons. The layer stacking is more perfect in graphitizing carbons than nongraphitizing. These apparent sizes and heights are important in the first stages of carbonization.
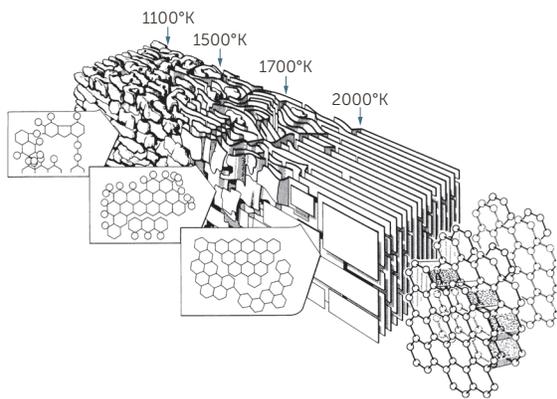

Figure 1-9. A model of changes from mesophase to graphite during heat treatment[3]

The structure of graphite with regard to interlayer spacings and crystallite size does change with temperature, Figure 1–9. Interlayer spacing, d, decreases as heat-treat temperature increases. Beginning at about 1500°C (2732°F), the interlayer spacing, d, decreases sharply from about 3.50 Å to about 3.40 Å when the temperature reaches 2000°C (3632°F). At this point it begins to level off, approaching 3.35 Å above 3000°C (5432°F). The crystallite size, La, increases as heat-treat temperatures increase.

Conversely to the interlayer spacing, d, the crystallite size, La, begins a sharp increase about 1500°C (2732°F) and continues to about 2000°C (3632°F) where it begins to level off. The size at <1500°C (2732°F) is 50 Å and increases to about 400 Å at 2000°C (3632°F).

A difference will be noted in petroleum coke versus pitch coke. The pitch coke does not increase to the same size as the petroleum coke at the same temperature. It parallels about 75 Å lower, beginning about 1700°−1800°C (3092°−3272°F). L_a is the basal plane size. La, which also increases, is the stacking direction height, Figure 1-5. The total size increases while the interlayer spacing, d, decreases. These changes, along with processing parameters, account for the excellent properties of petroleum coke-based graphite

DENSITY EFFECTS

Isotropy is independent of density. A high- or low-density material can be isotropic or anisotropic. The general crystal "structure" is also independent in that the greatest effects on density are due to process parameters. The same crystal "structure" can exist independently of the density of the bulk piece.

APPARENT DENSITY

DEFINITION

The density of a substance is the amount of material, or mass, per unit volume. Density is ordinarily expressed in grams per cubic centimeter or pounds per cubic foot (1 g/cm³ = 62.4 lb/ft³). To determine the density of a specimen, one would first calculate its volume from the physical dimensions (for a rectangular solid, the volume is equal to the product of the length, width, and thickness). Next, the mass would be determined by weighing the specimen. The density is determined by dividing the mass by the calculated volume.

If the specimen were completely homogeneous, with no flaws or voids, this method of determining density would yield the theoretical value. Graphite materials are, however, porous; hence, the term apparent density.

In general, the differences in graphite densities reflect what some of the other physical properties will be. The higher-density graphite will, generally, be stronger with a higher hardness value plus improvement in many other properties and characteristics.

The mathematical expression for the determination of density is:

$$D = \frac{W}{V}$$

Where: D = Density in g/cm³
    W = Weight of specimen in grams
    V = Volume of specimen in cm³

Or, if the weight is expressed in pounds and the volume is expressed in cubic feet, then the density would be in units of pounds per cubic foot.

Sample Calculation:

A graphite specimen has a length (l) of 1.000 inches, a width (w) and thickness (t) of 0.500 inches, and a weight of 7.500 grams. Calculate the apparent density (D).

$$V = l \cdot w \cdot t = 1.000 \text{ in} \cdot 0.5000 \text{ in} \cdot 0.5000 \text{ in}$$
$$V = 0.25 \text{ in}^3$$

To convert to cm³, multiply by 16.387 (1 inch = 2.54 cm, Appendix A).

$$D = \frac{W}{V} = \frac{7.500 \text{ g}}{4.097 \text{ cm}^3} + 1.831 \text{ g/cm}^3$$

TEST METHODS

The standard method commonly used to determine the apparent density of graphite is described in ASTM® Standard C559 and *Research & Development – Analytical Services Laboratory Instruction* (TDI) 4.1.1.1, Appendix B.

For premium graphites, such as our grades, the "water method" is an alternate method of determining apparent density. This method can be used on objects of irregular shape where the volume would be difficult to calculate. Even though the graphite is porous, the intrusion of water into the porosity is slow and the accuracy with this method is ±1 percent if the submerged weight is taken quickly.

The general steps in the "water method" are as follows:

1. Support the piece of graphite by a thin wire/thread and weigh the piece of graphite in air.

2. Submerge the piece in a container of water in such a way that the submerged weight can be determined.

3. Calculate the density by the following formula:

$$D = \frac{W}{W_1 - W_2} \times D_L$$

Where: D = Density in g/cm³
    W = Weight (in grams)
    W1 = Weight in air (in grams)
    W2 = Weight in water (in grams)
    DL = Density of water

APPARENT DENSITY COMPARISON TO CONVENTIONAL GRAPHITES

Our graphites are manufactured in a variety of grades covering the density range from 1.30 g/cm³ to 1.88 g/cm³. The density is a particularly important graphite characteristic because, in addition to its inherent significance, it has a direct influence on other properties. Generally, the physical and mechanical properties improve as the density is increased; details will be presented in later sections. Commercial polycrystalline graphites seldom exceed 80 percent of the theoretical density figure (2.26 g/cm³) due to voids and pores. Single crystal and pyrolytic graphites, because of their highly ordered structures and absence of pores, have densities closely approaching the theoretical value. In comparison to most other materials of construction, graphite has a low density, Figure 2-1. This is a decided advantage for some applications.

TEMPERATURE EFFECT

The apparent density will be influenced by temperature during the graphitization process. Generally, the higher the graphitization temperature, the higher the density will become. There are other factors which may contribute to this also, but there is an appreciable density increase as you go from 2000°C (3632°F) to 3000°C (5432°F).
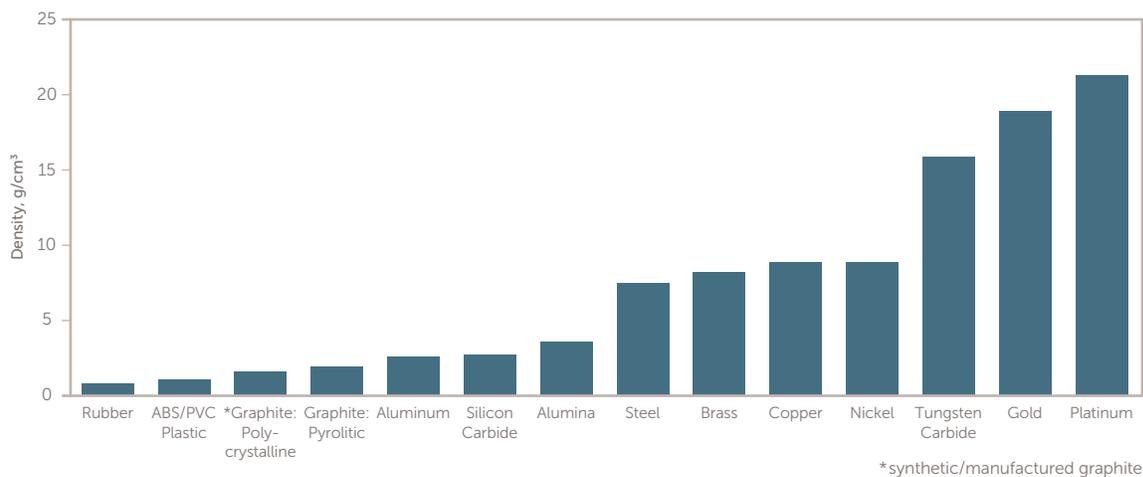
*synthetic/manufactured graphite

Figure 2-1. Typical densities of various engineered materials

POROSITY

DEFINITION

The standard definition for porosity, as found in ASTM Standard C709 which has definitions of terms relating to manufactured carbon and graphite, is "the percentage of the total volume of a material occupied by both open and closed pores." When one calculates the apparent density of a material, the pore volume is included in the calculation. This results in typical maximum densities for nonimpregnated manufactured graphites of 1.90 g/cm³. The theoretical density of graphite is 2.26 g/cm³. This means that in the very best case, about 16 percent of the volume of a bulk piece of graphite is open or closed pores. This porosity plays an important role in many ways, as will be discussed later.

The porosity characteristics of our finegrained graphites have been studied extensively.[4]

TEST METHODS

There is no recognized ASTM standard for measuring the porosity of manufactured graphites at this time. A number of techniques may be employed for the purpose and are widely in use today. It is important to state the method by which porosity data is determined because each method imparts its own bias.

One of the more widely used methods is mercury porosimetry. Two other methods in use are gas absorption by the BET technique and direct image analysis of the microstructure. The latter is gaining increased acceptance as a means of more accurately measuring the real pore structure. The advent of computer and video equipment has pushed this technique to the forefront of the porosimetry field. There are, nonetheless, limitations to this method also.

The mercury porosimetry technique is the method used for the data reported in our graphite literature. It involves basically pushing, under increasing pressure, mercury into the pores and as a function of pressure and volume filled, the pore size and pore volume can be determined. There are certain disadvantages of this method, such as:

1. The pores are not usually circular in cross-section and so the results can only be comparative.

2. The presence of "ink-bottle" pores or some other shape with constricted "necks" opening into large void volumes. The pore radius calculated by the Washburn equation is not truly indicative of the true pore radius and capillaries are classified at too small a radius.

3. The effect of compressibility of mercury with increasing pressure. This should be corrected for by carrying out a blank run.

4. The compressibility of the material under test. This is a problem of particular importance for materials that have pores that are not connected to the surface, e.g., cork. Additionally, pore walls may break under the pressures used if the material under test is relatively weak. This could cause a bias in the data.

5. The assumption of a constant value for the surface tension of mercury.

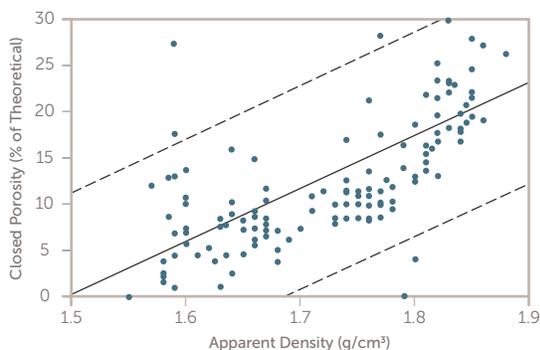6. The assumption of a constant value for the angle of contact of mercury.

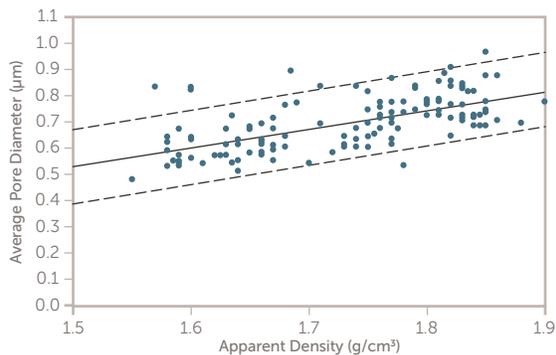*Figure 3-1. Closed porosity versus apparent graphite density*

Figure 3-2. Average pore diameter versus apparent graphite density

Entegris has carried out extensive analysis via mercury porosimetry to determine fundamental porosity parameters such as pore size and distribution, pore volume, and surface area. Using these pore characteristics, two basic linear correlations were observed: closed porosity versus graphite apparent density, Figure 3-1, and average pore diameter versus graphite apparent density, Figure 3-2.

The mercury porosimetry measurements were made on a Micromeritics® Mercury Porosimeter, Model 915-2.

A surface tension constant of 480 dynes/cm and a wetting contact angle of 140 degrees were assumed and used in the Washburn equation[5] where P is pressure in psi, r is the pore radius in cm, γ is the surface tension, and θ is the contact angle. A pressure and penetration volume reading were derived from the mercury porosimetry apparatus.

Penetration volume and pressure data were used to generate a printout of pressure, volume, pore size and percent porosity relationships. Graphical plots were generated to summarize pore size distribution information; percent porosity was plotted as a function of pore diameter.

$$Pr = -2\gamma \cos\theta$$

The surface area was also determined for each sample as described in the relationship[6] where S is the surface area in square meters per gram. In addition, the total closed porosity was determined from the theoretical porosity and the observed (open) porosity. Percent open and closed porosity were expressed as theoretical porosity.

$$S = 0.0225 \int_{0}^{V\,max} PdV$$

The above porosity parameters are displayed in graphical form as closed porosity versus apparent density and average pore diameter versus apparent density in Figures 3-1 and 3-2, respectively. Linear regression analysis was performed to determine the best fit equation (dotted lines represent limits at the 95 percent confidence level).

The results of these porosimetry studies indicate a linear relationship between average pore diameter and graphite apparent density. That is, as the graphite apparent density increases the average size of the pores increases. Previous in-house photomicrograph studies confirm this observation. Closed porosity was also found to increase with graphite apparent density. As can be predicted on the basis of the above surface area equation and the above observations, surface area varies inversely with graphite apparent density. A greater amount of surface area is observed in the lower-density graphite than in the higher-density product. At first glance, these observations are surprising and may even seem contradictory. Why should closed porosity increase when a concomitant increase in the pore diameter is also observed?

Although cause-and-effect relationships are difficult to establish, graphite porosity, pore size, and surface area are all physically related to density. Their relationship to density, whether direct or inverse, has implications on the structural properties of our graphite. The following physical model is advanced to rationalize the above relationships.

One notes that as graphite density increases, closed porosity and average pore size also increase while graphite surface area decreases. As the graphite structure increases in density, the smaller pores can be imagined to become more and more occluded until they are isolated from the rest of the pore system. As this process occurs, the smaller-diameter pores are systematically eliminated until only the larger, less complex pores remain. This also creates a larger amount of closed porosity. Thus, not only does the average pore diameter increase as a result of the elimination of small open pores, but pore surface area is reduced, since only pores with less branched structures remain.

Mercury porosimetry data on fine-grained graphites reveals a definite relationship between closed porosity and apparent density with the closed porosity increasing as the apparent density increases. The pore size also increases as apparent density increases.

POROSITY COMPARISON TO CONVENTIONAL GRAPHITE

The pore volume will be the same for all graphite with the same apparent density, but that is where the similarity ends. The pore diameter of our graphites range from 0.2 microns nominal to 0.8 microns nominal for our 1 and 5 micron grades and densities. The open porosity ranges from 75 percent open to 95 percent open and the pores are generally spherical in shape. The smaller pore size materials have a very large surface area associated with them. Conventional graphites will, at best, have typical pore sizes only down to several microns in size. The distribution of pore sizes is very narrow for our graphites, while they are generally broader for conventional graphites, Figure 3-3.

The fineness of the porosity allows our materials to be modified to create truly impermeable graphite. With various post-processing techniques, we can seal, fill, or close the porosity, depending on the end application. The high degree of open porosity also
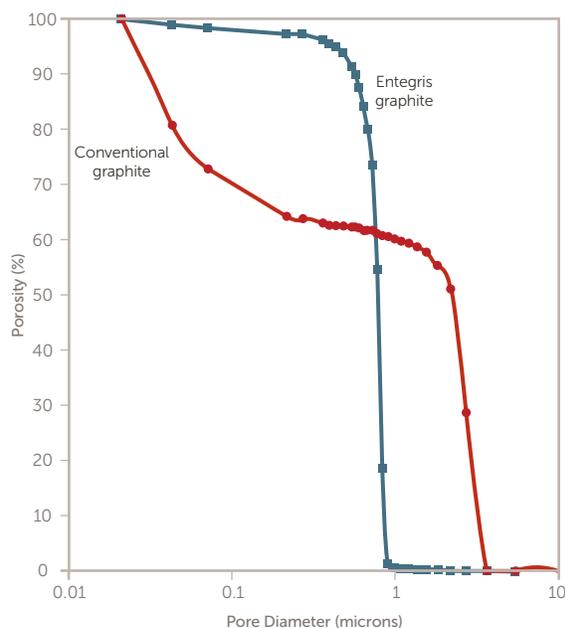

Figure 3-3. Open porosity % distribution graphite comparison

allows us to purify the material to less than 5 parts-per-million (ppm) total impurities, by ash analysis. Figure 3-4 shows helium flow data on various grades of our graphite. It clearly shows a wide variety of capabilities for graphites. The helium flow test for checking the permeability, like the mercury poro-simetry test, has its limits or bias and should be clearly identified when using data generated by it. Permea-bility is simply the rate of flow of a medium such as a gas or liquid through a material while under a pressure gradient. Our graphite pores are not only uniformly distributed, but are well interconnected so flow can take place through them. There are applications (such as filters) where this is important.

Another feature of the small pore size is that some liquids will not generally penetrate the pores readily. For instance, it has been determined that after soaking in water for seven days, a sample of AXF-5Q graphite picked up less than one percent by weight of the water, Figure 3-5. This could be an advantage in some applications. However, in other applications, such as wanting to infiltrate a liquid such as molten copper, very high pressures are required at high temperatures to accomplish it. This is a decided disadvantage.
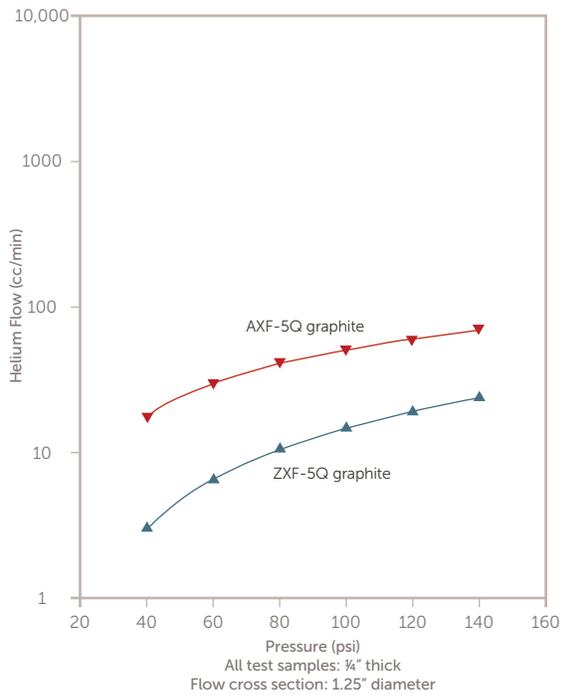
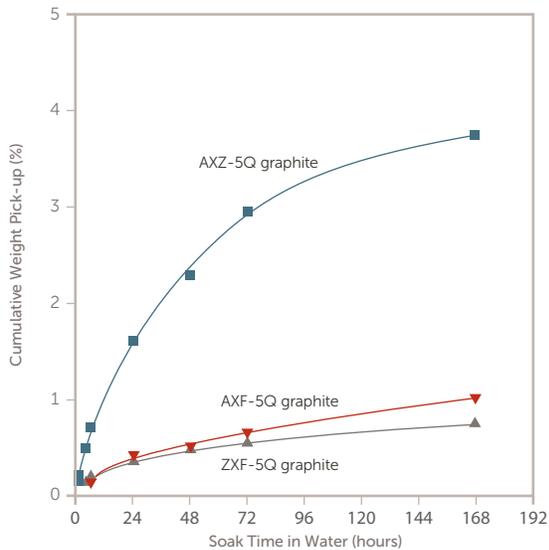Figure 3-4. Helium flow vs. pressure for some graphite materials

Figure 3-5. Water absorption of some graphite materials

TEMPERATURE EFFECTS

As temperature increases, pores will expand along with the rest of the matrix to the point of opening what were previously closed pores. As graphitization temperature increases, the pores will generally be found to be slightly smaller in size. It is uncertain what would happen to an impermeable graphite at room temperature if it were raised to very high temperature. Theoretically, if it is surface sealed, it may retain its impermeability. If it is densified, additional pores may open and thus render it permeable once more.

DENSITY EFFECTS

Mercury porosimetry data on fine-grained graphites reveals a definite relationship between closed porosity and apparent density with the closed porosity increasing as the apparent density increases. The pore size also increases as apparent density increases. The relationship is linear, with closed porosity increasing as density increases and pore size also increasing as density increases. If post-processing densification techniques were employed to raise the density, the pore size and pore volume would decrease.

HARDNESS

DEFINITION

Although the term "hardness" has comparative signifi-cance in an engineering sense, it is generally not considered to be a fundamental property of matter. The index of hardness is generally a manifestation of several related properties. In graphite, for instance, the particle size and porosity, and apparent density have an influence on the hardness value. The hardness value can be changed by the graphitization temperature as well, which generally relates back to a strength characteristic such as shear strength at the crystallo-graphic level. Different hardness testers are influenced by different properties and as a consequence cannot be correlated very well. Comparatively, soft materials may be hard in the sense that they can resist abrasion stresses, whereas harder materials in the sense of indentation hardness may fail completely under the same circumstances. It should be obvious at this point that the term "hardness" is relative and hardness data must be interpreted in relation to the type of hardness tests used.

An appropriate definition of hardness then would be the resistance of a material to permanent deformation of its surface. The deformation may be from scratching, mechanical wear, indentation or in a broader sense, cutting. Cutting would clearly include machinability as an index of hardness. This is much less precise than conventional hardness testers, but can be an indicator of relative usefulness.

TEST METHODS

There are two standard test methods for hardness of graphite: ASTM Standard C886, the Scleroscope Hardness method, and C748, the Rockwell Hardness method. Shore Scleroscope measures hardness in terms of the elasticity of the material. A diamondtipped hammer in a graduated glass tube is allowed to fall from a known height onto the specimen to be tested, and the hardness number depends on the height to which the hammer rebounds; the harder the material, the higher the rebound (see also Mohs hardness). Brinell hardness is determined by forcing a hardened steel or carbide ball of known diameter under a known load into a surface and measuring the diameter of the indentation with a microscope. The Brinell hardness number is obtained by dividing the load, in kilograms, by the spherical area of the indentation in square millimeters; this area is a function of the ball diameter and the depth of the indentation.

The Rockwell hardness tester utilizes either a steel ball or a conical diamond known as a brale, and indicates hardness by determining the depth of penetration of the indenter under a known load. This depth is relative to the position under a minor initial load; the corresponding hardness number is indicated on a dial. For hardened steel, Rockwell testers with brale indenters are particularly suitable; they are widely used in metalworking plants.

The Vickers hardness tester uses a square-based diamond pyramid indenter, and the hardness number is equal to the load divided by the product of the lengths of the diagonals of the square impression. Vickers hardness is the most accurate for very hard materials and can be used on thin sheets.

The Scleroscope hardness test method is based on the rebound height of a diamond-tipped hammer off the sample's surface after it falls a fixed distance. The scale is unitless, with the degree of hardness directly related to the height of the rebound. The higher the rebound, the "harder" the material. There are many

factors that affect the reproducibility and accuracy of the data. Studies at Entegris indicate that sample size, i.e., mass, has a significant bearing on the results as well. The results of a large billet will generally be higher than a small test sample.

The Rockwell hardness test method is based on the differential—the depth of indentation—produced on a sample's surface by a primary and secondary load and a specific-sized indenter. The hardness is taken directly from a dial reading. The higher the number, the "harder" the material. A variety of loads and indenter sizes are available depending upon the material being tested and its expected hardness. For graphite, the method specified calls for use of the "L" scale with a 60 kg load and a 6.35 mm diameter steelball indenter.

This works well for conventional graphites, but our Ultrafine particle graphites are usually off the scale on the high side when tested with this method. Another scale and/or a smaller indenter would be more appropriate, but a standard method has not been developed for use. However, a number of our customers specify use of the Rockwell 15T scale for hardness data. This is a 15 kg load with a 1.5875 mm diameter steel-ball indenter. There are a number of factors that affect the accuracy of this method, regardless of the scale used. They are listed in TDI 4.1.1.4, Section 3.4, Appendix B.

HARDNESS COMPARISON TO CONVENTIONAL GRAPHITES

Since hardness is influenced by a number of other factors, the comparison of our graphite to conventional graphites is relative at best. If all factors were held constant, including graphitization temperature and no artificial densification, etc., based strictly on particle size alone, our graphite would have a higher hardness number.

TEMPERATURE EFFECTS

Generally speaking, the higher the temperature, the softer or lower the hardness becomes. There is a direct relationship to graphitization temperature. The lower this temperature is, the higher the hardness number will be. As the temperature increases to about 3400°C (6152°F), the hardness will continue to slowly drop. From room temperature up to the material's original graphitization temperature, the hardness will show basically no change.

DENSITY EFFECTS

There is a correlation of hardness to density for the base graphite, Figure 4-1. As density increases, a general increase is seen in hardness. This is associated with the amount of porosity, which basically lowers the penetration resistance. The lower the density, the greater the pore volume and the less the resistance to the penetrator and, hence, a lower hardness number. If the porosity is filled with a material for densification purposes, the hardness might increase slightly. If, however, a material such as copper, which is very soft and ductile, is introduced into the pores, the overall hardness drops in direct relationship to the volume of copper filling the pores. Hence, a material with 75 percent open porosity will have a higher hardness when filled with copper than a material initially having 95 percent open porosity when it is filled with copper.
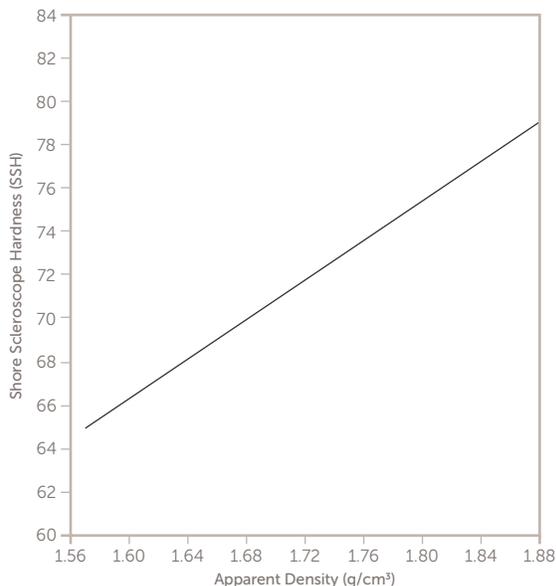

Figure 4-1. Correlation of hardness to density in our graphites

IMPACT TESTING

In standard testing, such as tensile and flexural testing, the material absorbs energy slowly. In real life, materials often absorb applied forces very quickly: falling objects, blows, collisions, drops, etc. Impact tests are performed to measure the response of a material to dynamic loading. Izod and Charpy are two methods used to investigate the behavior of specified specimens under specified impact stresses, and to estimate the brittleness or toughness of specimens. They should not be used as a source of data for design calculations on components. Information on the typical behavior of a material can be obtained by testing different types of test specimens prepared under different conditions, varying notch radius and test temperatures, etc.

DEFINITION

Impact energy for a material is the amount of energy, usually given in joules or foot-pound force, required to fracture a material, usually measured by means of an Izod or Charpy test. The type of specimen and test conditions affect the values and therefore should be specified.

TEST METHOD

Izod impact testing was performed per ASTM D256-97, modified for graphite specimens and for geometry (10 mm x 10 mm), using a Model CS-137-047 machine.

These test methods determine the material resistance to breakage by flexural shock as indicated by the energy extracted from "standardized" pendulum-type hammers, mounted in "standardized" machines, in breaking standard specimens with one pendulum swing. The standard tests for these methods require specimens made with a milled notch. In the Charpy and Izod tests, the notch produces a stress concentration that promotes a brittle, rather than a ductile, fracture. The results of all tests are reported in terms of energy absorbed per unit of specimen width.

Table 5.1: Izod impact strength of ACF-10Q (FT/LB)

	ACF-10Q GRAPHITE		ACF-10QE2 GRAPHITE	
Identification	NOTCHED	UNNOTCHED	NOTCHED	UNNOTCHED
1	0.095	0.748	0.107	0.721
2	0.084	0.479	0.108	0.708
3	0.078	0.597	0.112	0.570
4	0.081	0.371	0.113	0.639
5	0.086	0.430	0.104	0.598
6	0.091	0.690	0.105	0.780
7	–	0.539	–	0.681
8	–	0.558	–	0.612
9	–	0.652	–	0.650
10	–	0.503	–	0.788
11	–	0.650	–	–
Group Average	0.086	0.565	0.108	0.675

These results are based on the tests performed and are subject to change upon the receipt of new or additional information.

WEAR RESISTANCE

Material wear is a very complex phenomena that can be defined as damage to a solid surface, generally involving progressive loss of material, due to relative motion between that surface and a contacting substance or substances. Wear can be affected by the hardness of the two materials coming into contact, the load, the temperature, the rate of movement between the two surfaces, and the chemical environment. Wear mechanisms can be classified as abrasive, adhesive, fatigue, erosion, or corrosion.

DEFINITION

Wear is the process in which two moving surfaces come into contact with each other and material is removed from those surfaces due to the relative motion between them. The material may be removed from one or both of the surfaces. Wear may be measured using a number of techniques; each technique simulates a specific type of wear.

TEST METHOD

In the test reported here, the pin-on-disk test, a large force (the load) is concentrated onto a small surface area (the contact area of the pin or ball). The ball used (in this case 52100 steel) is harder than the material tested, so that the tested material, and not the ball, will wear. The pin-on-disk test simulates situations where a large force is concentrated on a small area. Because of that it is considered an accelerated test, in that the force seen by the tested material is typically much greater than would be seen in an actual application. In the tests reported here, a 10 N force (~1 kg load) was used on a contact area of ~0.1 mm^2.

Samples were tested by Advanced Refractory Technologies (ART), using a pin-on-disk (POD) tester manufactured by Spire Inc. Pin-on-disk is used to measure the wear on a surface. It specifically measures sliding wear due to two surfaces sliding against each other as opposed to abrasive wear, which is due to the action of abrasive particles.

In this test, a weighted ¼" diameter 52100 steel ball travels in a circular path on the surface. The test is run for 10,000 revolutions with a fixed load, either 5 or 10 N. When the test is complete, the wear is measured by measuring the cross-sectional area of the wear track using ART's Tencor P-10 profilometer. By multiplying this cross-sectional area by the track length, a wear volume (volume of material removed during the test) can be determined. The wear volume (in mm³) is divided by the distance the test ran (in m), and the load on the sample (in N), to obtain a wear factor.

The wear factor is expressed in units of mm³/Nm. The wear factor calculation is a useful method of quantifying the wear resistance of a surface, and for comparing different surfaces.

WEAR RESISTANCE COMPARISON TO OTHER MATERIALS

Two graphite samples supplied by Entegris were tested – ACF-10Q and ACF-10QE2 graphite. Two tests were run on each graphite sample. For comparison, tests were also run on high-density polyethylene (HDPE) and on Teflon® (PTFE). Test conditions are shown in Table 6-1; results are shown in Table 6-2. In Table 6-3, the average value of the two tests for each graphite sample is shown. Note that a lower wear factor indicates less wear (more wear resistance).

Table 6.1: Test conditions

Sample	Load	Number of revolutions	Track radius
ACF-1QE2A1	10 N	10,000	7.925 mm
ACF-1QE2A1	10 N	10,000	9.525 mm
ACF-10QB1	10 N	10,000	7.925 mm
ACF-10QB1	10 N	10,000	9.525 mm
HDPE	10 N	10,000	9.525 mm
PTFE	10 N	10,000	9.525 mm

Table 6.2: Test results

Sample	WEAR AREA (FOUR MEASUREMENTS)				Standard deviation	Wear factor
	A	B	C	D		
ACF-1QE2A1	1.27×10^{-3} mm³	3.16×10^{-3} mm³	3.25×10^{-3} mm³	2.50×10^{-3} mm³	9.14×10^{-4} mm³	2.55×10^{-5} mm³/Nm
ACF-1QE2A1	3.77×10^{-3} mm³	2.20×10^{-3} mm³	1.30×10^{-3} mm³	1.34×10^{-3} mm³	1.16×10^{-3} mm³	2.15×10^{-5} mm³/Nm
ACF-10QB1	5.51×10^{-4} mm³	1.64×10^{-3} mm³	5.12×10^{-4} mm³	1.24×10^{-3} mm³	5.94×10^{-4} mm³	9.85×10^{-6} mm³/Nm
ACF-10QB1	2.34×10^{-3} mm³	2.16×10^{-3} mm³	1.88×10^{-3} mm³	2.49×10^{-3} mm³	2.63×10^{-4} mm³	2.22×10^{-5} mm³/Nm
HDPE	6.03×10^{-3} mm³	6.35×10^{-3} mm³	4.97×10^{-3} mm³	5.31×10^{-3} mm³	6.36×10^{-4} mm³	5.66×10^{-5} mm³/Nm
PTFE	9.92×10^{-2} mm³	1.21×10^{-1} mm³	1.27×10^{-1} mm³	9.91×10^{-2} mm³	1.45×10^{-2} mm³	1.11×10^{-3} mm³/Nm

Table 6.3: Summary of results

Material	Average wear factor
Graphite ACF-1QE1	2.3×10^{-5} mm³/Nm
Graphite ACF-10Q	1.6×10^{-5} mm³/Nm
HDPE	5.7×10^{-5} mm³/Nm
PTFE	1.1×10^{-3} mm³/Nm

COMPRESSIVE STRENGTH

DEFINITION

The easiest strength characteristic of a material to understand and measure is the compressive strength. When a material is positioned between two flat, parallel platens and a continually increasing compressive force is applied, either of two things can occur:

1. If the material is ductile, such as copper or iron, atomic or molecular bonds can be re-formed easily; therefore, when crystalline planes begin to slip across each other, the atoms will readily re-form bonds with other atoms. Consequently, it is quite possible to flatten a very ductile material, such as gold, into a very thin sheet (if high enough compressive load is applied).

2. If the material is brittle, such as graphite or many ceramic materials, atomic or molecular bonds cannot be re-formed easily; therefore, when crystalline planes begin to slip, catastrophic failure occurs and the material fractures.

The compressive strength of a brittle material is expressed as the maximum force per unit area that can be withstood before failure occurs. It is usually expressed in pounds per square inch (lb/in² or psi) or in megapascal (MPa) in metric units. The mathematical expression for the determination of compressive strength is:

$$C.S. = \frac{L}{A}$$

Where: C.S. = Compressive strength
L = Load required to cause failure
A = Cross-sectional area of specimen

Sample Calculation:

A graphite specimen with a cross-sectional area of 0.25 square inches fails when a load of 3500 pounds is applied; calculate the compressive strength.

$$C.S. = \frac{L}{A} = \frac{3500 \text{ lbs}}{0.25 \text{ in}^2} = 14,000 \text{ psi}$$

To convert to MPa, multiply by 0.0068948.

Compressive strength = 97 MPa

NOTE: 1 psi = 0.0068948 MPa
Other units and the appropriate conversion factors are given in Appendix A.

TEST METHOD

The standard method of measuring the compressive strength of a graphite specimen is described in ASTM Standard C695. Our method differs in that the specimen used is rectangular rather than a right cylinder. Cushion pads are not used either (TDI 4.1.1.14 in Appendix B and Figure 7-1).
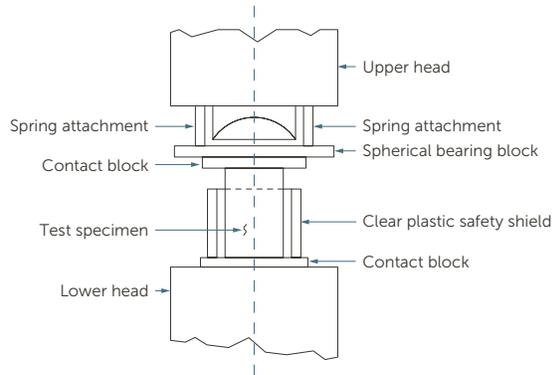

Figure 7-1. Elements of compressive strength load train

COMPRESSIVE STRENGTH COMPARISON TO CONVENTIONAL GRAPHITES

Our graphites have high compressive strengths compared to conventional materials. The compressive strengths of our materials range from 69 MPa (10,000 psi) to over 207 MPa (30,000 psi) depending on the grade selected. These values are two to three times higher than most other graphites. The final heat-treating temperature used in the manufacture of a carbon/graphite material has a marked effect on its compressive strength; the lower the final temperature, the higher the compressive strength.

TEMPERATURE EFFECTS

As the temperature of a piece of graphite is increased, its compressive strength increases, up to about 2500°C (4532°F). This is particularly important in such applications as hot pressing dies, where the material is subjected to both high temperature and high stress levels. Depending on the grade and type of graphite, compressive strength measured at 2500°C (4532°F) will increase from 15 to 50 percent over its room-temperature value.

The graphitization temperature also has a marked effect on the compressive strength. The lower the graphitization temperature, the less graphitic the material is and the higher the compressive strength will be. This is readily seen when comparing carbon-based material to graphite-based material for areas such as mechanical application.

DENSITY EFFECTS

As with many other properties, the compressive strength of graphites changes with apparent density; the higher density having the highest strength, Figure 7-2.
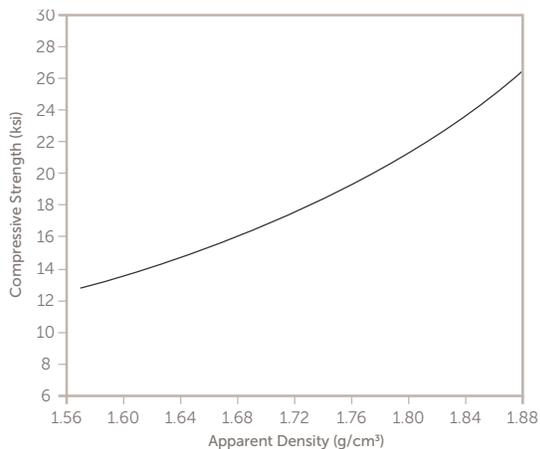

Figure 7-2. Compressive strength of the graphite changes when apparent density increases

FLEXURAL STRENGTH

___

DEFINITION

Flexural strength, tensile strength, and compressive strength are the three common tests performed to measure the strength of materials. In flexural strength testing, a steadily increasing bending movement is applied to a long bar until the material eventually ruptures. If the material is ductile (like copper), it will bend prior to breaking. However, if the material is brittle (such as chalk or graphite), it will bend very little before it fails catastrophically.

Flexural strength can be defined as the maximum stress in bending that can be withstood by the outer fibers of a specimen before rupturing, Figure 8-1.
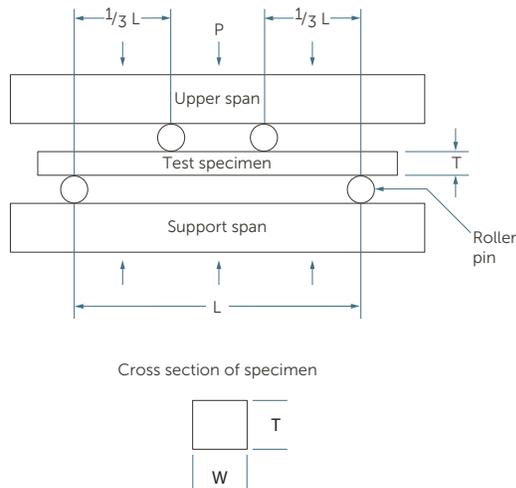

Figure 8-1. Four-point loading fixture

The mathematical expression for calculating flexural strength is:

$$F.S. = \frac{PL}{W(T)^2}$$

Where:
F.S. = Flexural strength in pounds per square inch (psi)
P = Load in pounds at failure
L = Length between outer support roller pins in inches
W = Width of specimen in inches
T = Thickness of specimen in inches

Sample Calculation:

Assume a graphite specimen 4.0 inches long by 0.75 inches wide by 0.50 inches thick is flexure tested on a fixture with support roller pins 3.0 inches apart. The specimen fails under a 500 pound load; calculate its flexural strength.

$$F.S. = \frac{PL}{W(T)^2} = \frac{500 \times 3.0 \text{ lbs}}{0.75 \times (0.50)^2} = \frac{1500}{0.1875 \text{ in}^2} \text{ psi} = 8000 \text{ psi}$$

To convert to MPa, multiply by 0.0068948.

Flexural strength = 55 MPa

TEST METHOD

The details of the procedure commonly used for testing the flexural strength of graphite are found in ASTM Standard C651. POCO's method (TDI 4.1.1.13 in Appendix B) differs in that the specimen geometry has a 1:1 ratio in thickness and width rather than the 2:1 width to thickness. The fixture used is not exactly as described either, but with a surface finish of less than 32 micro inches Ra on the sample, the frictional component is minimized, and results are comparable to those obtained with the fixture recommended by ASTM. Regardless of the procedure followed, steps must be taken to avoid factors that bias the results, such as improper sample alignment, rough and/or non-parallel surfaces. It is also important to know whether the reported strength values were obtained from three-point or four-point loading.

For example, a test specimen typically has a uniform rectangular cross section but the load may be applied in three or four point as illustrated in Figure 8-2. Note the shaded areas indicating the stress distribution. In three-point loading, the peak stress occurs on a single line at the surface of the test bar and opposite the point of loading. The stress decreases linearly along the length of the bar, and into the thickness of the bar, until reaching zero at the bottom supports.

Unlike the three-point bend tests, where the peak stress occurs on a single line opposite the point of loading, four-point loading distributes the peak stress over an area that is determined by the width of the sample and the span of the top loading supports, respectively. Observe how the tensile stress distribution decreases linearly from the area of peak stress on the tensile face, and into the thickness of the bar, until reaching zero at the bottom span supports. The increased area and volume under peak tensile stress, or near the peak tensile stress, in four-point loading increases the probability of encountering a larger flaw.

The probability of detecting the largest flaw in the specimen during three-point loading is minimized since the largest flaw must be at the surface and along the line of peak stress. Consequently, the specimen fractures at either a smaller flaw or within a region of lower stress, thus yielding artificially higher strength values in comparison with four-point loading results. The strength limit of the material, or even the local stress and flaw size that caused fracture, is not revealed in three-point loading. It only indicates the peak stress on the tensile surface at the time of fracture for a given material.
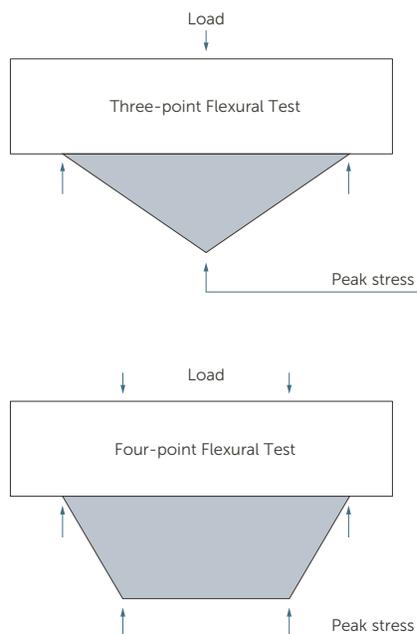

Figure 8-2. Four-point bend strength <three-point bend strength

FLEXURAL STRENGTH COMPARISON TO CONVENTIONAL GRAPHITES

In a brittle material such as graphite, the flexural strength is particularly sensitive to flaws or defects in the material. If a flaw is present within span L, i.e., between the outer support pins of the flexural test specimen, then the load P required to break the sample will be reduced. When failure occurs, it is catastrophic. The sample breaks suddenly and, frequently, small chips and flakes of material break away at the point of failure.

Our graphites have flexural strengths covering the range from 34 MPa (5000 psi) to over 124 MPa (18,000 psi). These values are quite high when compared to conventional graphites, which may range from less than 7 MPa (1000 psi) to around 41 MPa (6000 psi). The fine particle size and homogeneous structure of our graphites contribute to their high flexural strengths. Another important characteristic of this property in our graphites is that the flexural strength is the same for samples cut from any direction or orientation of the parent block of material. This characteristic is called isotropy; our graphites are said to be isotropic, whereas most other graphites are anisotropic. In conventional graphites that are molded or extruded, the ratio of flexural strengths between the "against grain" and "with grain" directions may range from 0.3 to 0.5.

TEMPERATURE EFFECTS

One of the unusual properties of graphite is that it gets stronger as it gets hotter (up to about 2500°C (4532°F). This is contrary to most materials, which lose strength as the temperature increases. The flexural strength of graphites will increase by 20 to 50 percent when the test temperature is increased from 25°C to 2500°C (77°F to 4532°F).

DENSITY EFFECTS

Flexural strength, like many other physical properties of graphite, increases with increasing density. For example, nominal flexural strength of 5 micron graphite (AXF-5Q, AXM-5Q, and AXZ-5Q) ranges from 6000 – 17,000 psi for densities of 1.60 (g/cm²) and 1.88 (g/cm²), respectively, Figure 8-3.
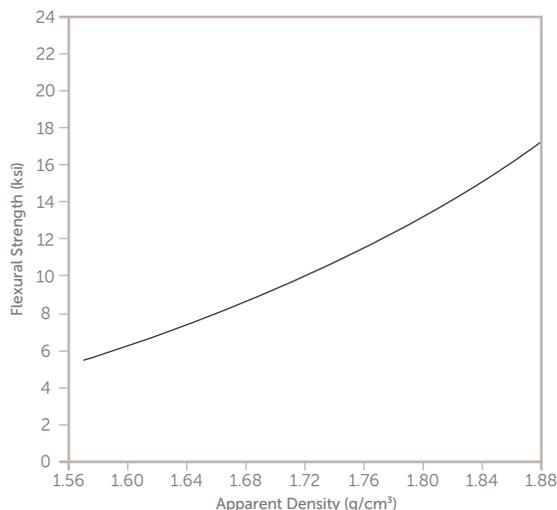

Figure 8-3. Nominal flexural strength vs. apparent density of AXF-5Q, AXM-5Q, and AXZ-5Q graphites

TENSILE STRENGTH
—

DEFINITION

The tensile strength of a material can be defined as its strength when a pulling force is applied along the length of a sample. If a cylindrical bar of uniform cross-section is subjected to a steadily increasing tensile ("pulling apart") force along its axis, the material will eventually rupture and tear apart when a large enough force is applied. It is extremely difficult to correctly determine the tensile strength of a brittle material, such as graphite.

The reason for this is that when brittle materials fail in tension, a crack originates at some point and is rapidly propagated across the specimen, causing catastrophic failure. Any imperfection in the material, such as voids, or surface scratches, will cause stress concentrations at that point. Since the stress at this point is higher than the overall average throughout the specimen, a crack will begin to propagate and premature fracture will occur. To alleviate this situation, carefully machined, highly polished specimens are used. Also, of no importance is the alignment of the gripping apparatus on the specimen. Even small misalignments could cause premature fracture, resulting in an erroneous (low) value for the tensile strength.

Tensile strength, like compressive strength, is expressed in pounds per square inch and is calculated in the same manner as compressive strength, i.e., the applied force at failure is divided by the cross-sectional area of the sample.

Sample Calculation:

If a rod with a cross-sectional area of 0.25 in² breaks at a load of 2000 pounds, then the tensile strength is 8000 psi.

$$\text{Tensile strength} = \frac{\text{Load}}{\text{Area}} = \frac{2000 \text{ lbs}}{0.25 \text{ in}^2} = 8000 \text{ psi}$$

To convert to MPa, multiply by 0.0068948.

Tensile strength = 55 MPa

TEST METHOD

The details of the commonly used method for tensile strength testing are shown in ASTM Standard C565. Other, more sophisticated testing equipment has been developed for this test; one of the better ones uses hemispherical air bearings instead of chain connectors to eliminate misalignment of the sample.

TENSILE STRENGTH COMPARISON TO CONVENTIONAL GRAPHITES

The tensile strength of a brittle material, such as graphite, is very sensitive to defects or imperfections in the material. The fine structure and uniformity of our graphites result in higher tensile strength as compared to conventional graphites. Typical tensile strength for conventional graphites ranges from 14 MPa (2000 psi) to 34 MPa (5000 psi), as compared to 34 MPa (5000 psi) to 69 MPa (10,000 psi) for our materials, Table 9-1.

Table 9-1. Typical ultimate tensile strengths of various materials

MATERIAL	ULTIMATE TENSILE STRENGTHS
Natural rubber	>4v (10^3 psi)
ABS/PVC plastic	3 – 6 (10^3 psi)
Graphite (polycrystalline)	2 – 10 (10^3 psi)
Aluminum (wrought)	13 – 98 (10^3 psi)
Silicon carbide	3 – 20 (10^3 psi)
Alumina (ceramic)	20 – 30 (10^3 psi)
Steel (wrought)	90 – 290 (10^3 psi)
Brass	34 – 129 (10^3 psi)
Copper	29 – 76 (10^3 psi)
Nickel	50 – 290 (10^3 psi)
Gold	19 – 32 (10^3 psi)
Platinum	18 – 30 (10^3 psi)

Figure 9-1. Ultimate tensile strength of AXF-5Q graphite

Figure 9-2. Graphitization temperature effect on tensile strength

TEMPERATURE EFFECTS

As the testing temperature of graphite is increased, its tensile strength increases; this is in sharp contrast to the behavior of metals, which show a decrease in strength as temperature increases. In an inert atmosphere (to avoid oxidation), the tensile strength of AXF-5Q graphite is almost 20,000 psi (138 MPa) at 2760°C (5000°F), as compared to 9150 psi (63 MPa) at room temperature, Figure 9-1. This dramatic change is characteristic of graphite materials, even though most grades do not show the 100 percent increase that our graphites exhibit.

The final heat-treat temperature of the graphite has a marked effect on its room temperature tensile strength: the lower the heat-treat temperature, the higher the strength. This is similar to the effect seen on other strength characteristics where the less graphitic materials are harder and stronger. The relationship between graphitization temperature and tensile strength is shown in Figure 9-2.
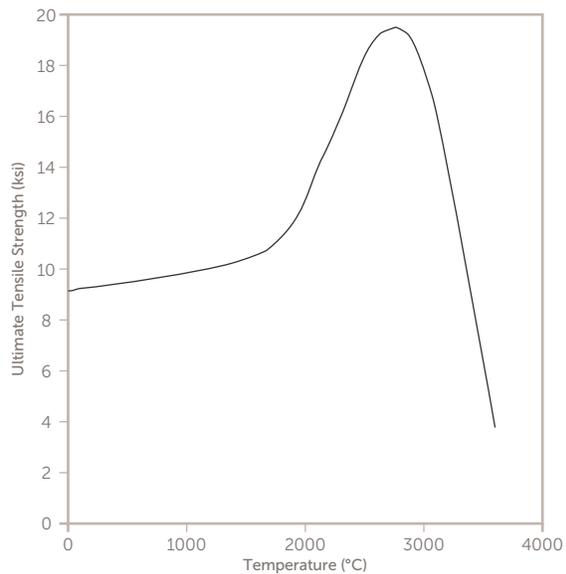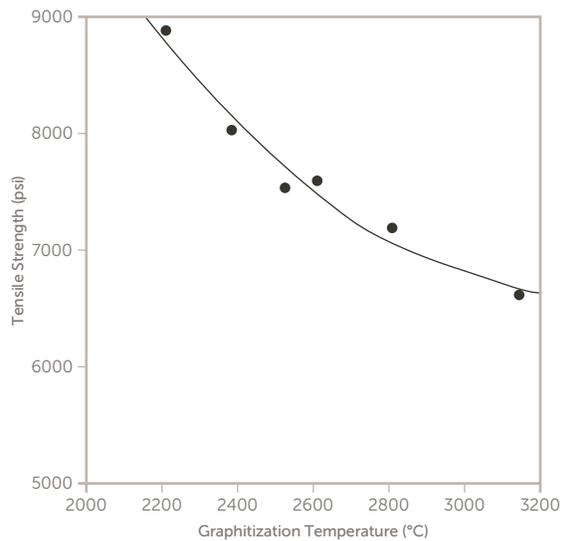
DENSITY EFFECTS

The tensile strength of graphite has a strong correlation with density: as the density increases, the tensile strength increases. This is typical of the other strength characteristics of graphites. Figure 9-3 shows the general relationship between density and tensile strength for the AXF-5Q, AXM-5Q and AXZ-5Q graphites. The nominal values of tensile strength range from 34 MPa (5000 psi) at 1.60 g/cm³ to 55 MPa (8000 psi) at 1.84 g/cm³.
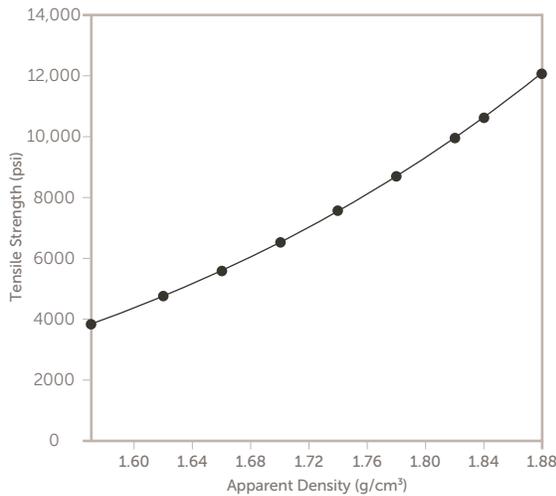

Figure 9-3. Nominal tensile strength vs. apparent density of AXF-5Q, AXM-5Q, AXZ-5Q graphites

MODULUS OF ELASTICITY
—

DEFINITION

The elasticity of a material is related to a uniformly increasing separation between the atoms of that material. As a consequence, the elasticity is directly related to the bonding between atoms and the respective energies associated therewith. This can be readily demonstrated by showing the general relationship between modulus of elasticity (MOE) and melting points of various materials. The higher the melting point (i.e., the energy required to disrupt the atom to atom bonds), the higher the modulus of elasticity, Figure 10-1. The presence of a second phase of differing modulus results in most of the stress being carried by the higher modulus phase. Porosity, which is uniformly distributed and continuous, constitutes a second phase. The effect on the modulus in materials of less than 50 percent pore volume can be represented by the relationship:

$$E_o (1 - 1.9P + 0.9P^2)$$

Where: P = Porosity (volume fraction)
E_o = Original modulus of elasticity

Another way of expressing the modulus of elasticity is by referring to Hooke's law, which applies to materials below their elastic limit. Basically, Hooke's law says that the average stress is proportional to the average strain.
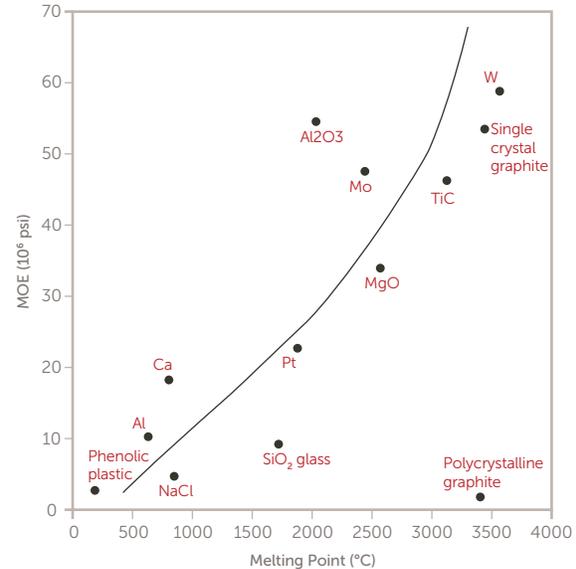

Figure 10-1. Modulus of elasticity vs. melting point for various materials

$$\frac{T}{e} = E = \text{Constant}$$

Where: T = Stress
e = Strain
E = Modulus of elasticity, or Young's modulus

Stress is the load per unit area and strain is the ratio of change in length to the original length, i.e.,

$$T = \frac{P}{A} \qquad e = \frac{\delta L}{L_o}$$

Where: P = Load
A = Area
δL = Change in length ($L - L_o$)
L_o = Original length

Therefore:

$$E = \frac{P / A}{\delta L / L_o} = \frac{PL_o}{\delta L}$$

Sample Calculation:

If a tensile sample with a diameter of 0.220 inch and a gage length of 1.000 inch breaks at 500 pounds with a gage length increase of 0.008 inch, the tensile MOE would be 1.6×10^6 psi.

$$E = \frac{PL_o}{\delta LA} = \frac{(500 \text{ lbs})(1)}{(0.008 \text{ in})(0.038 \text{ in}^2)} = 1.6 \times 10^6 \text{ psi}$$

The modulus of elasticity is usually expressed in millions of pounds per square inch (106 psi), or in N/mm^2 in metric units.

TEST METHOD

The standard method of measuring modulus of elasticity for graphite when not determined from samples tested in tension is described in ASTM Standards C747 and C769. The methods are approximations derived from other properties. A more accurate, but also more difficult, means is to attach proper strain measuring gages to tensile strength samples and measure strain along with stress during a tensile test. Then, employing Hooke's law, the modulus can be calculated.

MODULUS OF ELASTICITY COMPARISON TO CONVENTIONAL GRAPHITES

The modulus of elasticity varies for the many different grades of graphite available; therefore, a significant difference in the modulus for our materials compared to conventional graphite is not seen, Table 10-1. The most notable difference, however, is the isotropy of our graphite which assures a modulus of the same value in any direction as compared to many conventional graphites whose modulus changes depending on test orientation.

TEMPERATURE EFFECTS

As with the other strength properties of graphite, as temperature increases, the modulus of elasticity also increases, to a point beyond which it begins to drop rapidly. This is typically around 2500°C (4532°F). The increase can be as much as 25 percent higher before the drop begins. The final graphitization temperature also has an effect, but is relatively small.

Table 10-1. Modulus of elasticity of various graphites

	MATERIAL	APPARENT DENSITY	MOE
Entegris	AXZ-5Q	1.65 (g/cm³)	1.3 (10^6 psi)
	AXM-5Q	1.72 (g/cm³)	1.5 (10^6 psi)
	AXF-5Q	1.77 (g/cm³)	1.6 (10^6 psi)
Mersen®	2161	1.66 (g/cm³)	1.3 (10^6 psi)
	2020	1.77 (g/cm³)	1.3 (10^6 psi)
	2080	1.87 (g/cm³)	1.8 (10^6 psi)
Morgan	P3W	1.60 (g/cm³)	1.4 (10^6 psi)
	L-56	1.63 (g/cm³)	.5 (10^6 psi)
	P5	1.72 (g/cm³)	2.4 (10^6 psi)
	P03 1	0.82 (g/cm³)	1.8 (10^6 psi)
SGL Group, The Carbon Company®	H-440	1.75 (g/cm³)	1.5 (10^6 psi)
	HLM	1.75 (g/cm³)	1.8 (10^6 psi)
	H-463	1.75 (g/cm³)	1.8 (10^6 psi)
	H478	1.75 (g/cm³)	2.2 (10^6 psi)
Toyo Tanso USA®	SEM5	1.80 (g/cm³)	2.4 (10^6 psi)
	SEM3	1.85 (g/cm³)	1.4 (10^6 psi)
UCAR®	AGSR	1.58 (g/cm³)	1.6 (10^6 psi)
	CBN	1.67 (g/cm³)	1.8 (10^6 psi)
	CS	1.70 (g/cm³)	2.0 WG* (10^6 psi)
			1.1 AG* (10^6 psi)
	CBN	1.67 (g/cm³)	1.8 (10^6 psi)

* Shows typical anisotropy effects

DENSITY EFFECTS

The density relationship is evident with about a 15 to 20 percent increase in modulus detected as the density increases from 1.65 g/cm³ to 1.77 g/cm³. This follows the same pattern as other strength properties for graphite.

ELECTRICAL RESISTIVITY
—

DEFINITION

The electrical resistivity is that intrinsic property of a material that determines its resistance to the flow of an electrical current. The electrical resistance of a substance is directly proportional to the length of the current path, i.e., as the current path increases, the resistance increases. It is also inversely proportional to its cross-sectional area, i.e., as the area increases, the resistance decreases. The mathematical expression for the determination of electrical resistivity is:

$$ER = \frac{AR}{L}$$

Where: ER = Electrical resistivity at room temperature
A = Cross-sectional area (square inches)
R = Electrical resistance of the material (ohms)
L = Distance between potential contacts (inches)

Sample Calculation:

For a graphite sample with a cross-sectional area of 0.25 in², distance between the potential contacts of 2.0 inches and an electrical resistance reading of 0.00425 Ω (ohms); calculate the electrical resistivity.

$$ER = \frac{(0.25 \text{ in}^2)(0.00425 \text{ }\Omega)}{2.0 \text{ in}}$$

ER = 0.000531 Ω•in
ER = 531 μΩ•in
To convert to μΩ•cm, multiply by 2.54
Electrical resistivity = 1349 μΩ•cm

TEST METHOD

The standard method of measuring the electrical resistivity of a graphite sample is described in ASTM Standard C611. At Entegris only two resistance readings are taken, using a special sample holder with eight electrical contacts which takes the equivalent of four readings at once. We use test method TDI 4.1.1.2 (Appendix B).

ELECTRICAL RESISTIVITY COMPARISON TO CONVENTIONAL GRAPHITES

Our graphites have electrical resistivity values that fall into the range of most conventional graphites. Our graphites have a range from around 450 μΩ•in to 1050 μΩ•in. This may be compared to copper which has a range of 1.1 to 1.5 μΩ•in or tool steels which range from 7.1 to 7.5 μΩ•in. See Table 11-1 for other common material resistivities.

Table 11-1. Typical electrical resistivity of various materials*

Material**	Electrical Resistivity Range (μΩ•in)	Comments
Entegris graphites	450 – 1000	Polycrystalline graphite
Toyo Carbon graphites	300 – 600	Polycrystalline graphite
Mersen graphites	550 – 1200	Polycrystalline graphite
Toyo Tanso USA graphites	400 – 500	Polycrystalline graphite
Copper	1.1 – 1.5	Pure, wrought
Gold	0.9	Pure
Silver	0.6	Pure
Tungsten	2.2	Pure
Carbon steels	7.1 – 7.5	Hardening grades, wrought
Stainless steel	15.7 – 28.3	400 series, wrought
Cobalt base superalloys	36.6 – 74.3	Wrought
Nickel base superalloys	3.0 – 52.4	Wrought and cast
Silicon	6×10^6	Semiconductor
Silicon carbide	4×10^6	Semiconductor
Silicon nitride	4×10^{20}	Insulator
Alumina	$>4 \times 10^{21}$	Insulator

* Measured at room temperature in accordance with ASTM Standard C611 and TDI 4.1.1.2.
** Select samples from each manufacturer but not all-inclusive

TEMPERATURE EFFECTS

Electrical resistivity varies with temperature,[7] Figure 11-1. As the temperature increases from room temperature to about 700°C (1292°F), the electrical resistivity decreases. From that point, however, as the temperature increases, the resistivity also increases.
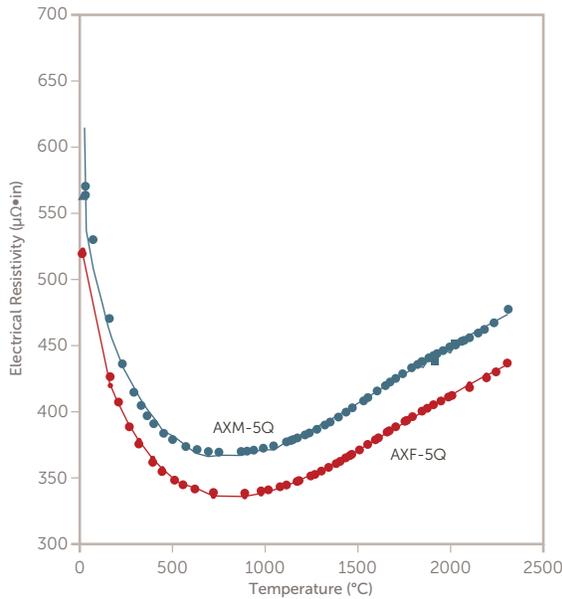
Figure 11-1. Electrical resistivity vs. temperature of AXM-5Q and AXF-5Q graphite

Graphitization temperature also has an effect on electrical resistivity. The higher the graphitization temperature, the lower the electrical resistivity becomes, as measured at room temperature.

DENSITY EFFECTS

Density is a particularly important characteristic of graphite because, in addition to its inherent significance, it has a large and direct influence on other properties. As the density of our graphite increases, its electrical resistivity decreases, Figure 11-2.
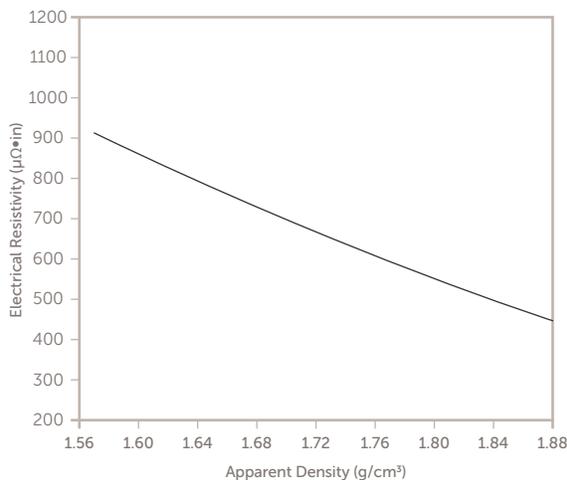

Figure 11-2. Nominal electrical resistivity of AXF-5Q, AXM-5Q, and AXZ-5Q graphites vs. apparent density

THERMAL EXPANSION

DEFINITION

The physical dimensions of a body are determined by the number and spacing of its atoms. At temperatures above 0 K, the atoms are always in constant vibration about their positions in the lattice. If energy is added to the material (by heating it), the atoms vibrate more vigorously, causing the macroscopic dimensions of the material to increase.

The coefficient of thermal expansion (CTE) is defined as the change in length of a substance per unit length for a specific change in temperature. If this thermal expansion is hindered in any way, internal stresses will occur.

When two different materials are to be joined permanently, as in the electrical connection to an incandescent lamp or a vacuum tube, it is important that they have nearly the same values of CTE if there is to be no danger of failure from cracking. The same precaution applies to coatings or cladding of one material to another.

The CTE is normally expressed as inch per inch per °C or as inch per inch per °F, with the temperature range over which the CTE is applicable being specified. This is done because, for some materials, the CTE will change with temperature.

The mathematical expression for the determination of the coefficient of thermal expansion is:

$$CTE = \frac{\delta L}{L(T_2 - T_1)}$$

Where: CTE = Coefficient of thermal expansion
δL = Change in sample length from the lower temperature to the upper temperature
L = Sample length at the lower temperature
T_1 = Lower temperature
T_2 = Upper temperature seen by sample

Sample Calculation:

A two-inch graphite sample is heated from room temperature to 1000°C (1832°F).

The length uniformly increases until it is 2.0164 inches in length at 1000°C (1832°F); calculate the CTE.

$$CTE = \frac{2.0164\ \text{in} - 2.0000\ \text{in}}{2.0000\ \text{in}\ (1000° - 23°C)}$$

CTE = 8.39×10^{-6} (in/in)/°C

To convert to (in/in)/°F: divide by 1.8

CTE = 4.65×10^{-6} (in/in)/°F

TEST METHOD

The standard method of measuring the coefficient of thermal expansion of a graphite sample is similar to ASTM Standard E228, but there is no specific method for graphite. We have a horizontal silica (orton) dilatometer and follow TDI 4.1.1.5 (Appendix B).

THERMAL EXPANSION COMPARISON TO CONVENTIONAL GRAPHITES

Our graphites have high coefficients of thermal expansion compared to conventional materials, Table 12-1. The coefficient of thermal expansion of our materials range from 7.0×10^{-6} to 9.0×10^{-6} (in/in)/°C, depending on the grade selected. These values are two to four times higher than most other graphites.

Table 12-1. Coefficient of thermal expansion

MATERIAL	10^{-6} (IN/IN)/°C	
	HIGH	LOW
Aluminum alloys (68–212°F)	24.1	22.3
300 Stainless steels (32–212°F)	18.7	14.9
Copper (68–572°F)	17.6	16.7
Nickel base superalloys (70–200°F)	17.8	10.6
Cobalt base superalloys (70–1800°F)	17.1	16.2
Boron nitride (70–1800°F)	7.5	–
Titanium carbide (77–1472°F)	7.4	6.7
Tungsten carbide	7.4	4.5
Silicon carbide (0–2550°F)	4.3	3.9
Silicon nitride (70–1800°F)	2.5	–
Entegris graphite (70–1832°F)	8.8	7.0

TEMPERATURE EFFECTS

As the temperature of a piece of graphite is increased, its coefficient of thermal expansion will become greater, Figure 12-1. There is limited data to describe its expansion characteristics above 1000°C (1832°F), but the data available indicates a linear increase in expansion as high as 2500°C (4532°F).
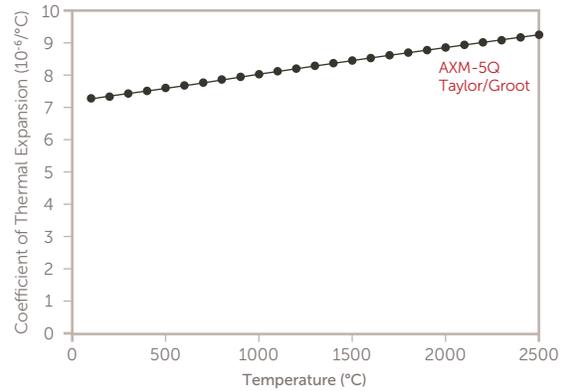

Figure 12-1. CTE vs. temperature of AXM-5Q graphite

DENSITY EFFECTS

As with many other properties, the coefficient of thermal expansion changes with apparent density; as the density of the material increases, so will the coefficient of thermal expansion.

Since the higher-density material has less porosity, there is less distance for the crystals to move unobstructed as the temperature is increased; therefore, higher density means greater expansion, Figure 12-2.
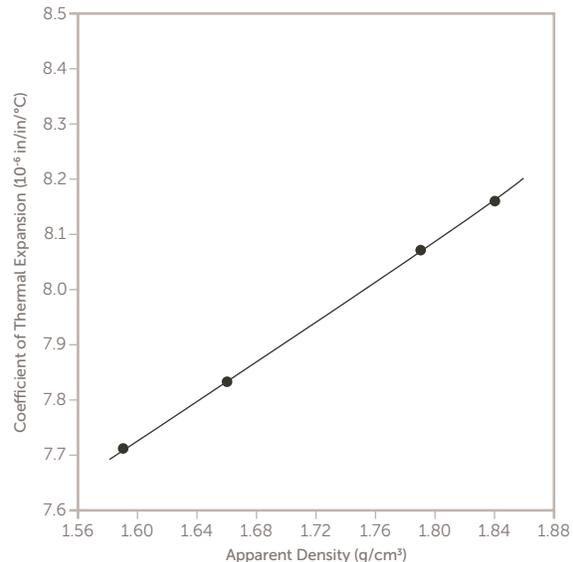

Figure 12-2. CTE vs. apparent density of AXF-5Q, AXM-5Q, and AXZ-5Q graphite

THERMAL CONDUCTIVITY

DEFINITION

The thermal conductivity of a material is a measure of its ability to conduct heat. A high thermal conductivity denotes a good heat conductor, while a low thermal conductivity indicates a good thermal insulator, Table 13-1.

Table 13-1. Typical thermal conductivity of various materials

MATERIAL	THERMAL CONDUCTIVITY RANGE BTU•FT/HR/FT² °F
Natural rubber	0.082
Nickel	6 – 50
Steel (wrought)	8 – 21
Silicon carbide	9 – 25
Tungsten carbide	16 – 51
Brass	15 – 135
Iron (cast)	25 – 30
Enetgris graphite	40 – 70
Platinum	42
Conventional graphite	65 – 95
Aluminum	67 – 135
Tungsten	97
Copper	112 – 226
Gold	172
Silver	242

The mathematical expression for thermal conductivity (K) is:

$$K = \frac{Q\partial X}{A\partial T}$$

Where: Q = Rate of heat flow through a slab in BTU per hour
A = Cross-sectional area of the slab in feet²
∂X = Thickness of slab in feet
∂T = Temperature drop across the slab (°F)

Therefore, K is expressed as:

BTU•ft/hr/ft² °F
or
cal/(meter °C sec)
or
W/m•K

Sample Calculation:

Assume a flat plate of graphite 0.1 foot thick has a surface area of one square foot. Heat is flowing through this plate at a rate of 1000 BTU per hour; the hotter surface is at a temperature of 1036°F, while the cooler surface is at 1018°F; calculate the thermal conductivity.

$$K = \frac{Q\partial X}{A\partial T} = \frac{(1000\ BTU)(0.1\ ft)}{(hr)(1\ ft^2)(1036°F - 1018°F)}$$

$$K = \frac{(1000\ BTU)(0.1\ ft)}{(hr)(1\ ft^2)(18°F)} = 55.5\ \frac{BTU•SSft}{hr/ft^2\ °F}$$

To convert to metric system of units, multiply by 0.413 to obtain:
K = 22.9 cal/(meter °C sec)

To convert to SI system of units, multiply by 1.73 to obtain:
K = 96.0 W/m-K

TEST METHOD

Historically, two different techniques were employed for determining thermal conductivity over the temperature range of 110 – 3300 K. They are:

1. A comparative rod apparatus from 110 K to 1250 K

2. A radial inflow apparatus from 1250 K to 3300 K

There is no standard method associated with graphite for measurement of thermal conductivity.

However, ASTM Standard C714-72 is routinely used for determining thermal diffusivity and the corresponding results are used to calculate thermal conductivity. Our graphite deviates from ASTM Standard C714-72 in that this standard requires the use of a flash lamp for sample heating and thermocouples for monitoring temperature. We employ a similar technique using a Netzsch® LFA-427 (Laser Flash Apparatus) that has a high-intensity laser to heat the sample surface and the resultant temperature change is monitored with an infrared detector, Figure 13-1.
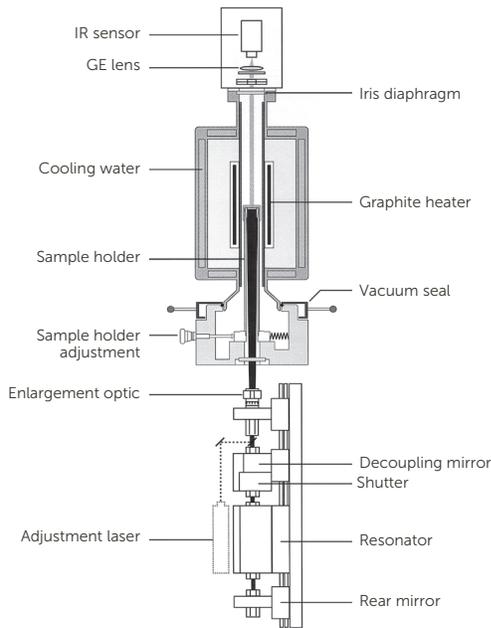
Figure 13-1. Netzch LFA-427

Thermal diffusivity measurements involve quantifying the rate of diffusion of heat through a solid where local temperature and temperature gradients vary with time. This is a decided advantage in that thermal diffusivity measurements are nonsteady-state, due to the transient nature of diffusion, thus eliminating the need for determining heat flux and maintaining steady-state conditions. Nonetheless, close control of local time-temperature relationships in the system is required. Thermal diffusivity methods are also preferred over heat flux measurements due to the ease of sample preparation. With less material requirements and fast measurements, one typically obtains accuracy within ±5% when implementing careful measurement techniques. Thermal conductivity is calculated from the relationship:

$$K = aC_P\rho$$

Where: K = Thermal conductivity (W/cm•K)
α = Thermal diffusivity (cm²/sec)
C_P = Heat capacity at constant pressure (J/g K)
ρ = Apparent density (g/cm³)

THERMAL CONDUCTIVITY COMPARISON TO CONVENTIONAL GRAPHITES

From studies on our graphite and experimental work on other graphites, it is believed that the conductivity of most graphites is mainly governed by Umklapp type phonon-phonon interactions.

For our graphite and most other graphites, thermal conductivity begins to decrease around 27°C (70°F) and continues to decrease as the temperature increases to 3227°C (5840°F). Thermal diffusivity and thermal conductivity results for our graphite grades are indicated in Figures 13-2 and 13-3, respectively, as a function of temperature from 23° – 1650°C (73° – 3002°F).

It has been reported that above 2727°C (4940°F), electrons contribute about 20 percent to the total thermal conductivity of these graphites. For more highly graphitized graphites and other feedstocks, the results can be different
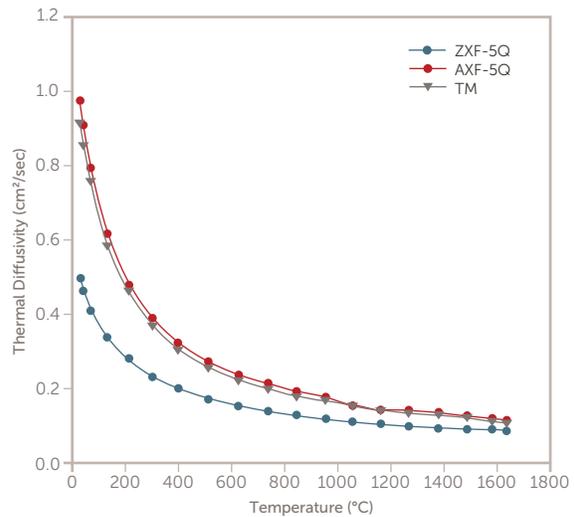

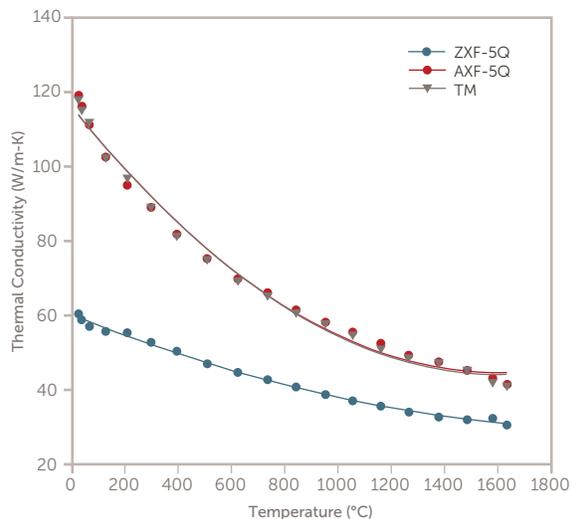*Figure 13-2. Thermal diffusivity of various graphites*

Figure 13-3. Thermal conductivity of various graphites

DENSITY EFFECTS

The density of graphite is significant in its effect, as on the other properties. As the density of our graphite increases, its thermal conductivity also increases.

THERMAL SHOCK
—

Definition

The ability of a material to be subjected to sudden thermal gradients without weakening or fracturing is referred to as its thermal shock resistance. The excellent resistance of graphite to thermal shock is due to a unique set of properties. High strength, low modulus of elasticity, and low coefficient of thermal expansion are the properties that are most important. This theoretical relationship can be expressed as:[8]

$$R = \frac{\sigma_f(1-\varnothing)}{aE}$$

Where: R = Thermal shock resistance
σ_f = Fracture stress
$\varnothing$ = Poisson's ratio
α = Coefficient of thermal expansion
E = Modulus of elasticity

This relationship applies only when the quench is so fast that the surface temperature reaches final value before the average temperature changes.

For conditions when the heating rate is not very high, a second relationship can be established that includes thermal conductivity. This is expressed as:

$$R' = \frac{\sigma_f(1-\varnothing)K}{aE}$$

Where: R' = Thermal shock resistance
σ_f = Fracture stress
$\varnothing$ = Poisson's ratio
K = Thermal conductivity
α = Coefficient of thermal expansion
E = Modulus of elasticity

Another way to express this would be:

$$R = \frac{KT_s}{aE_T}$$

Where: R = Thermal shock resistance
K = Thermal conductivity
T_s = Tensile strength
α = Coefficient of thermal expansion
E_T = Tensile modulus of elasticity

This expression may be a simpler form to use and consequently will be used in the sample calculation.

In either case, the typical properties of carbon and graphite generally yield the best overall thermal shock resistance of all the temperature-resistant, non-metallic materials available. This is useful for rocket nozzle and re-entry nose-cone applications, among others.

Sample Calculation:

A graphite sample with a thermal conductivity of 0.29 (cal cm)/(cm² sec °C) and a tensile strength of 10,000 psi (703 kg/cm²) has a modulus of elasticity of 1.6×10^6 psi (0.112×10^6 kg/cm²) and a CTE of 8.4×10^{-6} (in/in)/°C; calculate its thermal shock resistance.

$$R = \frac{KT_s}{aE_T} = \frac{\dfrac{0.29 \text{ cal} \times \text{cm}}{\text{cm}^2 \times \text{sec} \times °C}}{\dfrac{8.4 \times 10^{-6}}{°C}} \cdot \frac{\dfrac{703 \text{ kg}}{\text{cm}^2}}{\dfrac{0.112 \times 10^{-6} \text{ kg}}{\text{cm}^2}}$$

$$R = 216.7 \frac{\text{cal}}{\text{cm} \times \text{sec}}$$

TEST METHOD

There are no standard test methods for accurately measuring the thermal shock resistance of materials. A number of practical tests are being used for specific applications. One such testing device is described by Sato.[9] Use of the relationships previously described is generally accepted for predicting thermal shock resistance of a material, but many other considerations must be made such as sample size, stress distribution in material (i.e., geometry and stress duration).

THERMAL SHOCK COMPARISION TO CONVENTIONAL GRAPHITES

Some early studies[10] reported that coarse-particle graphite had better thermal shock resistance than finer-particle graphite despite the higher strength of finer-particle graphite. The study further indicated a correlation to the binder. If the binder were decreased, the thermal shock resistance also dropped, suggesting the thermal stresses were being absorbed by the binder material. Other studies[11] have shown the precursor material, e.g., tar coke versus oil coke, to have effects on the thermal shock resistance. The oil coke had resistance values about seven times higher than the tar coke.

Generally, due to small particle size and high CTE, our graphite may not fare as well as some other graphites in overall thermal shock resistance. Tests at Entegris have shown that samples of the AXF-5Q grade graphite, measuring one inch cubed, can survive a 1000°C to 10°C (1832°F to 50°F) instantaneous change without fracturing in repeated tests. Other tests on our graphites have subjected the samples to 168°C to -204°C (335°F to -335°F) instantaneous changes without affecting the graphite. A comparison of thermal shock resistance values for some materials is shown in Table 14-1.

Table 14-1. Thermal shock resistances

		CAL/CM•SEC
Enetgris graphites	(AXF-5Q)	217
	(ZXF-5Q)	233
GLC	(Graphnol)	450
Mersen graphite	(2020)	140
Pyrolytic graphite	(w/grain)	4300
	(a/grain)	0.29
SGL Group, The Carbon Company graphite	(EK-82)	252
	(EK-87)	426
Titanium carbide	(unknown)	3.45
Toyo Tanso USA graphite	(Isograph 88)	340
UCAR	(ATJ)	329

While the differences are not as great between the various grades as the pyrolytic graphite shows between orientations, it should still be noted that processing variables, starting materials, etc., can influence the thermal shock resistance of graphite. For example, the Ringsdorff EK-87 grade has an average particle size of 20 microns, yet it has about 30 percent more calculated thermal shock resistance than the UCAR ATJ, which has an average particle size of 25 microns and nearly twice the calculated resistance of our graphite with a particle size average of 4 microns.

TEMPERATURE EFFECTS

Depending on the type of graphite used and its particular characteristics or properties, and considering shape, size, etc., higher temperature drops could be sustained without affecting the graphite. The temperature starting and ending points may have some bearing on the overall resistance to fracture, because the material will be thermally stressed differently at elevated temperatures. A drop from 1000°C to 500°C (1832°F to 932°F) may respond differently than from 500°C to 0°C (932°F to 32°F). Little data is available to clearly define what the relationship or limits are for the different graphite types.

DENSITY EFFECTS

Since, generally, strength and thermal conductivity increase with density, higher thermal shock resistance should be found in higher-density ranges. However, with higher density, higher modulus and CTE are also usually found and these would tend to offset the gains in strength. The coarser-particle systems may be more effective than the finer-particle systems on an equal density basis. Many factors are involved, and well defined tests to measure these effects are not in common use.

SPECIFIC HEAT
—

DEFINITION

Heat capacity is the quantity of heat required to raise the temperature of a unit mass of material 1°, and the relationship between the two most frequently used units is as follows:

$$1 \frac{BTU}{lb\ °F} = 1 \frac{cal}{g\ °C}$$

It has been found that the values of heat capacity for all types of natural and manufactured graphites are basically the same, except near absolute-zero temperatures. The differences found in measuring the same grade of graphite are as great as the differences in measuring different grades of graphite. Differences as much as nine percent have been found between natural graphite and manufactured graphite at low temperatures (120 K to 300 K), but at higher temperatures the differences for all types of graphite has been found to be less than the experimental error. Table 15-1 shows comparisons to other materials.

HEAT CAPACITY EQUATION

The heat capacity at constant pressure (C_p) can be expressed by polynomial functions of the absolute temperature T, with T in K to give CP in cal/(g°C).

Within the temperature interval 0 K to 300 K:

$$CP = (0.19210 \times 10^{-4})T - (0.41200 \times 10^{-5})T^2 - (0.10831 \times 10^{-7})T^3 - (0.10885 \times 10^{-10})T^4$$

However, below 40 K, this equation has not been reliable in correlation with experimental data. The calculated values are in good agreement (<2.2 percent) with the experimental values for temperatures above 40 K.

Table 15-1. Typical specific heat of various materials

MATERIAL	Heat Capacity Range cal/(g°C)	Heat Capacity Range J/(g K)
Gold	0.031	0.13
Platinum	0.031	0.13
Tungsten	0.034	0.14
Tungsten carbide	0.04	0.17
Silver	0.056	0.23
Brass	0.090	0.38
Nickel	0.091 – 0.14	0.38 – 0.59
Copper	0.092	0.38
Steel (wrought)	0.11	0.46
Iron (cast)	0.13	0.54
Graphite	0.17	0.72
Alumina	0.19	0.79
Aluminum	0.22 – 0.23	0.92 – 0.96
Silicon carbide	0.285 – 0.34	1.19 – 1.42

For the temperature range 300 K to 3200 K:

$$C_p = 0.44391 + (0.30795 \times 10^{-4})T - (0.61257 \times 10^{5})T^{-2} + (0.10795 \times 10^{8})T^{-3}$$

This expression yields calculated values within 1.5 percent of the experimental values for the entire temperature range.

Table 15-2. Typical specific heat of manufactured graphites

TEMPERATURE (K)	SPECIFIC HEAT (CAL/[G°C])	SPECIFIC HEAT (J/[G K])
0	0.0000	0.0000
50	0.0101	0.0423
100	0.0335	0.1402
150	0.0643	0.2690
200	0.0995	0.4163
250	0.1357	0.5678
300	0.1723	0.7214
350	0.2090	0.8750
400	0.2450	1.0258
450	0.2760	1.1556
500	0.3030	1.2686
550	0.3230	1.3523
600	0.3400	1.4235
650	0.3560	1.4905
700	0.3700	1.5492
750	0.3820	1.5994
800	0.3930	1.6454
850	0.4020	1.6831
900	0.4090	1.7124
950	0.4150	1.7375
1000	0.4210	1.7626
1100	0.4320	1.8087
1200	0.4430	1.8547
1300	0.4520	1.8924
1400	0.4600	1.9259
1500	0.4680	1.9594
1600	0.4740	1.9845
1800	0.4860	2.0348
2000	0.4960	2.0766
2200	0.5040	2.1101
2400	0.5110	2.1394
2600	0.5160	2.1604
2800	0.5210	2.1813
3000	0.5270	2.2064
3200	0.5360	2.2441
3400	0.5480	2.2944
3600	0.5800	2.4283
3800	0.6900	2.8889

Table 15-2 represents the best fit of the values for typical manufactured graphite with proper consideration given to the accuracy of the individual measurements.

Sample Calculation:

Determine the heat capacity of a sample of graphite at 500°C (932°F) using a differential scanning calorimeter (DSC) and a strip chart recorder to follow the calorimetric response for the temperature scans of 30°C (86°F). DSC scans are taken for the sample of graphite, a sapphire reference sample and the baseline for correction of the measured response. The heat capacity, C_P is then calculated for the graphite using the formula:

$$C_P \text{ (graphite)} = \frac{W_S}{W_G} \times \frac{D_S}{D_G} \times C_P \text{ (sapphire)}$$

Where: W_S = Weight of sapphire
W_G = Weight of graphite
D_S = Signal displacement of sapphire
D_G = Signal displacement of graphite

Let the weight of the sapphire reference = 0.203 g and a sample of AXF-5Q graphite, i.e., indicating a density of 1.82 g/cm³ and measuring 1.5 mm × 6 mm diameter, weigh 0.077 g, respectively. C_P of sapphire is 0.19 cal/ (g°C). C_P of graphite at 500°C (932°F) can be calculated by knowing the displacement as determined from the strip chart recorder.

Assume the displacement (corrected) is 40.0 for the graphite and 52.5 for the sapphire reference.

Therefore:

$$C_P \text{ (graphite)} = \frac{0.023 \text{ g}}{0.077 \text{ g}} \times \frac{40}{52.5} \times 0.19 \, \frac{cal}{g \, °C}$$

$$C_P \text{ (graphite)} = 0.382 \, \frac{cal}{g \, °C} = 1.6 \, \frac{J}{g \, K}$$

TEST METHOD

The previous example best illustrates how a DSC and a chart recorder may be used in determining heat capacity. However, modern technology has integrated the DSC with computer and software technology, thereby eliminating the need for calculating CP from a chart recorder. We currently use a Netzsch STA-449 Heat Flux DSC, Figure 15-1, for evaluating graphite and other related materials. Heat capacity calculations are made via software but the fundamental principles remain the same.
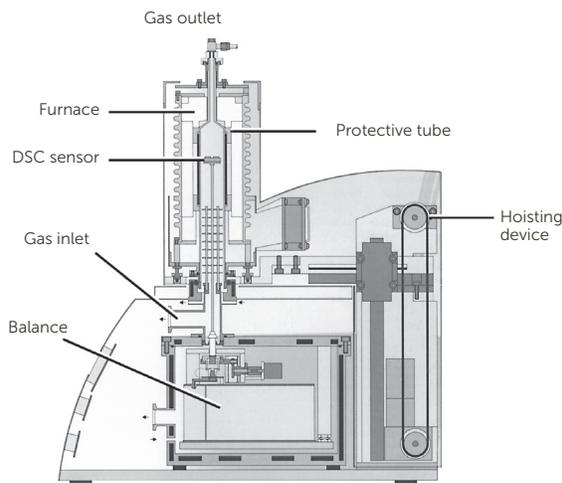

Figure 15-1. Netzsch STA-449

In DSC, a distinction must be made between the recorded baseline in the presence and absence of a sample. Thus, measurements are first taken with an empty sample crucible to determine the instrument baseline. A second run is made to verify the accuracy of the instrument by placing a sapphire reference sample in the sample crucible and taking measurements under the same experimental conditions. The DSC curve rises linearly resulting from the change in heat capacity of the sample as a function of temperature. Sapphire is routinely used as a reference material since it is stabilized, i.e., will not oxidize, and due to the fact that heat capacity for sapphire has been thoroughly investigated and well documented. Once the baseline and accuracy have been established, a third run is made on the sample of interest under the same experimental conditions.

There is no standard test method for determining specific heat of graphite, but the DSC method is commonly used for specific heat determination of other materials.

Another simple method that yields approximate specific heat data is an ice calorimeter. If a body of mass (m) and temperature (t) melts a mass (mL) of ice, its temperature being reduced to 0°C (32°F), the specific heat of the substance is:
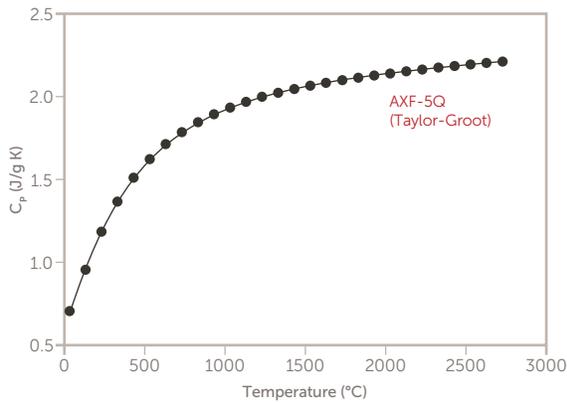
Figure 15-2. Specific heat vs. temperature: AXF-5Q graphite

SPECIFIC HEAT COMPARISON TO CONVENTIONAL GRAPHITES

Our graphites have heat capacity values that are in the same range as conventional manufactured graphites. Our graphites have a range from around 0.72 J/(g K) to 1.60 J/(g K) between 20° and 500°C (932°F), Figure 15-2.[12]

TEMPERATURE EFFECTS

The heat capacity of manufactured graphite increases with increasing temperature, Figure 15-3.

DENSITY EFFECTS

Heat capacity has no significant change as a function of density. It is intrinsic to the graphite crystal itself and apparently independent of density.
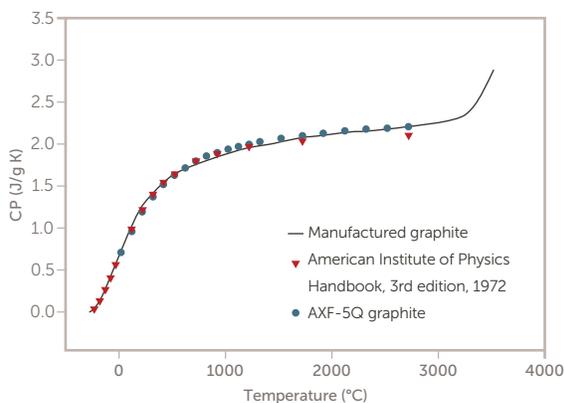

Figure 15-3. Specific heat of manufactured graphite

EMISSIVITY

DEFINITION

A measure of the heat radiating ability of a surface is referred to as emissivity. Total emissivity or spectral emissivity are ways to express it. The total emissivity is defined as the ratio of thermal energy emitted by a material per unit time per unit area to that emitted by a black body over the entire band of wavelengths when both are at the same temperature. A black body, i.e., ideal radiator, is one that absorbs all the radiant energy falling on it and, at a given temperature, radiates the maximum amount of energy possible over the entire wavelength spectrum.

The spectral emissivity is defined as the ratio of thermal energy emitted by a material per unit time per unit area to that emitted by a black-body reference where radiation from both are of the same wavelength and both are at the same temperature. The spectral emissivity of graphite has been measured at 6500 Å. Dull surfaced graphite and polished graphite have had typical values of 0.90 and 0.77, respectively. It has been determined that the emissivity of graphite does vary slightly with temperature. A temperature coefficient of $1.9 \times 10\text{-}5/K$ has been determined. Graphite emissivity has been found to be nearly constant in the wavelength range 2000 Å to 60,000 Å. Spectral emissivity values approaching 0.99 have been measured for graphite near sublimation temperatures of 3600 K. For a specific temperature, at a specific wavelength, normal spectral emissivity can be expressed as:

$$E_{n,\lambda} = \frac{W_{S,\lambda}}{W_{BB,\lambda}}$$

Where:
$W_{S,\lambda}$ = Normal spectral radiant energy emitted by a specimen material per unit time, unit area and unit solid angle.
$W_{BB,\lambda}$ = Normal spectral radiant energy emitted by a black-body reference per unit time, unit area, and unit solid angle.

$$\log E_{n,\lambda} = \frac{C}{2.303\lambda} \left[\frac{1}{T} - \frac{1}{T_{A,\lambda}} \right]$$

Normal spectral emissivity written as a function of temperature is:

Where: C = 14,380 micron − K
λ = 0.65 micron
T = Temperature of material (K)
$T_{A,\lambda}$ = Apparent temperature of material (K)

For a specific temperature the total normal emissivity can be expressed as:

$$E_{n,\lambda} = \frac{W_S}{W_{BB}}$$

Where:
W_S = Normal total radiant energy emitted by a specimen material per unit time, unit area and unit solid angle.
W_{BB} = Normal total radiant energy emitted by a black body reference per unit time, unit area and unit solid angle.

Total normal emissivity at elevated temperatures can be expressed as:

$$E_{n,t} = \frac{T^4_{A,t}}{T^4}$$

Where: T = Temperature of material (K)
$T_{A,t}$ = Apparent temperature of material (K)

Emissivity data has usefulness in applications such as aerospace, heaters, pyrometry, etc., but published data is difficult to find.

TEST METHOD

There are no standard methods for measuring emissivity of graphite, but one method used to measure the emissivity of graphite is described by Grenis and Levitt.[13] A schematic of this equipment can be seen in Figure 16-1. The methods of measuring emissivity are wrought with difficulties and results may be biased due to equipment and/or assumptions made in running the tests. At best, the testing is at a research level and not a routine procedure.
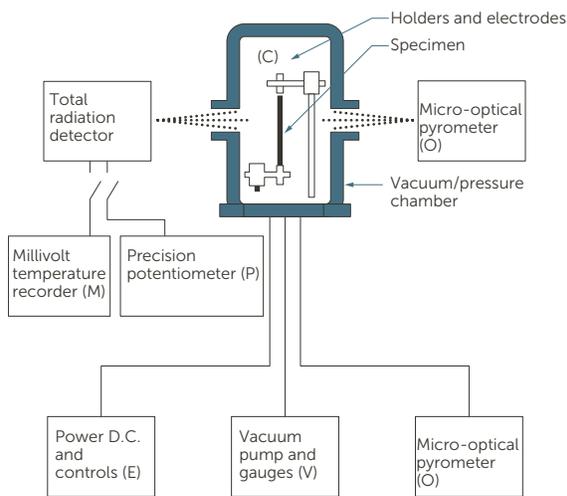

Figure 14-1. Schematic block diagram of the emissivity apparatus

EMISSIVITY COMPARISON TO CONVENTIONAL GRAPHITES

Very little information on the emissivity of graphite is available. The following information on total emittance of two grades of graphite and pyrolytic graphite has been reported by Cezairliyan and Righini.[14]

The equation for total emittance of AXM-5Q graphite as a function of temperature, between 1800 to 2900 K is:

$$E = 0.679 + (6.00 \times 10^{-5})T$$

The equation for AXF-5Q graphite, between 1700 to 2900 K is:

$$E = 0.794 + (2.28 \times 10^{-5})T$$

The equation for pyrolytic graphite, between 2300 to 3000 K is:

$$E = 0.641 - (5.70 \times 10^{-5})T$$

Where: T is in K.

Table 16-1. Total emittance

TEMPERATURE	AXM-5Q GRAPHITE	AXF-5Q GRAPHITE	PYROLYTIC GRAPHITE
1700 K	–	0.833	–
1800 K	0.787	0.835	–
1900 K	0.793	0.837	–
2000 K	0.799	0.840	–
2100 K	0.805	0.842	–
2200 K	0.811	0.844	–
2300 K	0.817	0.846	0.510
2400 K	0.823	0.849	0.504
2500 K	0.829	0.851	0.499
2600 K	0.835	0.853	0.493
2700 K	0.841	0.856	0.487
2800 K	0.847	0.858	0.481
2900 K	0.853	0.860	0.476
3000 K	–		0.470

The measured values of the total emittance of the graphite specimens are shown in Table 16-1 and again graphically in Figure 16-2.
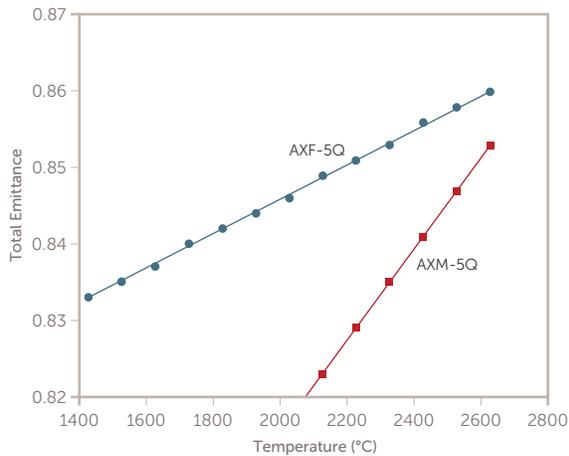
Figure 16-2. Total emittance of AXF-5Q and AFM-5Q graphite

The differences may be associated with layer plane orientation or other crystallographic effects, particularly when comparing a pyrolytic graphite to a polycrystalline graphite such as AXM-5Q. The difference seen between AXF-5Q and AXM-5Q graphites may go back to a surface roughness effect, but are primarily associated with the porosity differences with regard to size and frequency distribution across the surface.

ASH

DEFINITION

ASTM Standard C709 defines ash of manufactured carbon and graphite as the "residual product following oxidation of the base carbon as determined by prescribed methods." This ash or residual product generally results from natural contamination of the raw material used to produce graphite and may be introduced to a lesser extent during processing of the raw material or graphite products. Table 17-1 shows a general listing of typical elements and their level of contamination in graphite bulk product. As will be discussed later, there are means by which the contamination can be reduced or removed.

Table 17-1. Typical purity analysis standard Entegris graphite grades (unpurified) total ash range 300 – 1000 ppm

ELEMENT	ELEMENT DETECTED	PPM RANGE
Vanadium (V)	Yes	100 – 500
Iron (Fe)	Yes	5 – 300
Nickel (Ni)	Yes	1 – 100
Calcium (Ca)	Yes	5 – 100
Silicon (Si)	Yes	5 – 50
Aluminum (Al)	Yes	10 – 50
Titanium (Ti)	Yes	1 – 50
Potassium (K)	Yes	1 – 20
Sodium (Na)	Yes	1 – 15
Copper (Cu)	Yes	1 – 10
Magnesium (Mg)	Yes	1 – 5
Chromium (Cr)	Yes	Trace to 10
Phosphorus (P)	Yes	Trace to 10
Boron (B)	Yes	1 – 5
Sulfur (S)	Yes	1 – 5
Molybdenum (Mo)	Yes	Trace
Zinc (Zn)	Yes	Trace
Lithium (Li)	Yes	Trace

TEST METHOD

The standard test method for ash content of graphite is ASTM Standard C561. This technique applies principally to nonpurified graphites of several hundred ppm, or more, of total impurities. The method is generally too crude for good reproducibility on high-purity samples.

One disadvantage of this method is the potential loss of low melting point impurities due to the temperature at which the test is run. Theoretically, at 950°C (1742°F) as a final test temperature, nothing should be lost that was not already volatilized during graphitization, but as a practical matter, it seems to occur. These are possibly impurities trapped in closed pores that did not success-fully escape during the graphitization cycle. The test temperature could be lowered to preclude some of this from occurring, but then the time to complete the test is extended considerably as oxidation is a time-tempera-ture dependent reaction.

It has also been found in previous studies that at higher temperatures (desirable for shorter test cycles) reactions of carbon and platinum, of which the crucibles are made, can occur and consequently bias the test results.

Our method, TDI 4.1.1.6 (Appendix B), differs slightly from the ASTM procedure, in that a solid sample is used rather than a powdered sample. The risk of contamination in powdering the sample is nonexistent if a solid sample is used. A standard test cycle for nonpurified material is 24 hours, whereas, a purified material usually takes 48 – 72 hours to complete the cycle.

Sample Calculation:

If a graphite sample weighed 80.0000 grams after drying and was ashed in a 35.0000 grams crucible where the total ash after testing was 0.4 milligrams, the total ash would be 5 ±1 parts per million:

$$\text{Ash (ppm)} = \frac{C - A}{B - A} \times 1,000,000 =$$

$$\frac{35.0004 - 35.000}{115.0000 - 35.000} \times 1,000,000 = 5 \pm 1 \text{ ppm}$$

Where: A = Crucible weight
B = Crucible plus dried sample weight
C = Crucible plus ash weight

If ash % is required, multiply by $\frac{C - A}{B - A}$ 100
Ash % = 0.0005

ASH COMPARISON TO CONVENTIONAL GRAPHITES

When discussing nonpurified graphites, our graphites are fairly clean, i.e., contain relatively low levels of impurities. However, since graphitization temperature has a strong bearing on the impurities that remain, the ash levels on any product can vary accordingly. There are other process steps that influence the final ash level also.

In material that has been impregnated for densifica-tion, contaminants in the raw material used could increase the impurity content as well.

Our graphites will typically range from 300–3000 ppm total impurities, depending on the grade and density. Many conventional graphites fall within this range also, but some will be in the range of 0.1 percent (1000 ppm) to several percent (20,000–30,000 ppm).

Our purified graphite will have less than 5 ppm total impurities. This is one of the best grades of purified graphite available anywhere. The unique nature of the pore structure and relatively clean raw materials aids in allowing this ultra-high purity. Typical analysis of a purified graphite is seen in Table 17-2. Purified graphites can be produced in several ways. Simply heat-treating to very high temperatures, usually in excess of 3000°C (5432°F), will volatilize most heavy elements present. Halogen gases, such as chlorine or fluorine, will react with the impurities at high tem-perature and volatilize off as chloride or fluoride salts. Some elements such as boron are very stable and difficult to remove, especially since they can substitute for carbon atoms in the crystal structure.

TEMPERATURE EFFECTS

The only real temperature effect on ash levels comes from the graphitization temperature or a subsequent thermal processing to remove impurities. As men-tioned previously, the higher the final thermal treat-ment, the lower the ash level will usually be.

DENSITY EFFECTS

In our graphite, a slight trend has been noted with ash as related to density. Since our graphites have increasingly more open porosity as the density decreases, more opportunity for volatilization escape of the impurities during graphitization can occur. Consequently, slightly lower ash levels are typically found for the lower-density grades. This may be unique to our graphites. The difference is relatively small though, so it is mentioned only in passing, as a number of other factors may have more significant effects on the final ash level.

Table 17-2. Typical purity analysis purified Entegris graphite grades total ash range 5 ppm or less

ELEMENT	ELEMENT DETECTED	PPM RANGE
Silicon (Si)	Yes	Trace
Sulfur (S)	Yes	Trace
Vanadium (V)	Yes	Trace
Calcium (Ca)	Yes	Trace
Boron (B)	Yes	Trace
Aluminum (Al)	Yes	Trace
Magnesium (Mg)	Yes	Trace
Iron (Fe)	Yes	Trace
Molybdenum (Mo)	Yes	Trace
Phosphorus (P)	Yes	Trace
Nickel (Ni)	No	–
Titanium (Ti)	No	–
Potassium (K)	No	–
Sodium (Na)	No	–
Copper (Cu)	No	–
Chromium (Cr)	No	–
Zinc (Zn)	No	–
Lithium (Li)	No	–

OXIDATION

DEFINITION

Oxidation is a chemical reaction that results in electrons being removed from an atom, which makes the atom more "reactive" so that it may join with one or more other atoms to form a compound. When talking about carbon and graphite, oxidation is normally thought of as the reaction of carbon atoms with oxygen to form carbon monoxide (CO) and carbon dioxide (CO_2). However, many other gases (besides oxygen) will react with carbon in an oxidation reaction (e.g., CO_2, H_2O, N_2O, etc.). The result of the oxidation reaction is a loss of carbon atoms from the carbon or graphite material, which obviously affects many of its properties and characteristics. If oxidation of a piece of carbon is allowed to continue long enough, all the carbon atoms will react to form a gas (or gases) that dissipates and

leaves behind nothing except a small amount of ash, which is the oxides of the metallic impurities that were present in the carbon to begin with.

The oxidation of carbon by oxygen (as well as other gases) is highly temperature-dependent. No detectable reaction occurs at temperatures up to about 350°C (662°F). As the temperature is increased, the rate of reaction increases rapidly, according to the well-known Arrhenius expression:

$$\ln K \alpha E/RT$$

Where: T = Temperature
E = Activation energy
K = Reaction rate
R = Universal gas constant

TEST METHOD

To measure the oxidation characteristics of a particular carbon material, a piece of known weight is exposed to the "oxidizing environment" of interest for some period of time, and then reweighed, to determine a weight loss (the oxidation weight loss). There is not a widely accepted standard test for measuring the oxidation characteristics of carbon materials (TDI 4.1.1.7 and 4.1.1.8 in Appendix B).

The oxidation characteristics of carbon are usually expressed in one of two different ways:

1. The percent weight loss in 24 hours at a given temperature, often referred to as oxidation resistance

2. The temperature at which a sample loses approximately one percent of its weight in a 24-hour period, which is called the oxidation threshold temperature of the material being tested

Sample Calculation:

If a sample originally weighed 10.0000 grams after being dried and 9.9900 grams after oxidation testing, the percent weight loss would be 0.1 percent.

$$\%WT_L = \frac{WT_O - WT_F}{WT_O} \times 100 =$$

$$\frac{10.0000 - 9.9900}{10.0000} \times 100 = 0.1\%$$

Where: WT_O = Initial sample weight (dried)
WT_F = Sample weight after oxidation testing percent
WT_L = Percent weight loss

OXIDATION COMPARISON TO CONVENTIONAL GRAPHITES

The oxidation characteristics of any graphite at the same temperature and atmospheric conditions are dependent on the amount of impurities in the material, the density of the material and the amount of surface area available to react with the oxidizing atmosphere. Our graphites can be impregnated with a proprietary oxidation inhibitor that can substantially increase its oxidation resistance. Purification also reduces oxidation significantly by removing metallic impurities that act as oxidation catalysts.

As the surface area increases, the oxidation rate increases, too. This is expected, as the surface exposure is important to the oxidation process. For purposes of standardization and to minimize the effect of variable surface area to volume (SA/V) ratios, we use a sample with an SA/V ratio of 10:1 for testing oxidation rates.

TEMPERATURE EFFECTS

The differences in oxidation behavior of the various grades of graphite are widest at the lowest temperatures, tending to disappear as the temperature increases. The "oxidation threshold temperature," defined as that at which a sample loses approximately one percent of its weight in 24 hours, is about 570°C (1058°F) for purified graphite, while nonpurified graphite is about 430°C (806°F), Figure 18-1.

The oxidation of graphite is highly temperature dependent. At temperatures up to about 350°C (662°F), no detectable oxidation occurs. As the temperature is increased, the rate of reaction increases rapidly, according to the Arrhenius equation, Figure 18-2.

DENSITY EFFECTS

Since the oxidation of graphite is a surface reaction, it is known that the rate of oxidation is affected by the porosity of the material. As the percent porosity increases, the apparent density of the material will decrease. Therefore, as the apparent density decreases, the rate of oxidation will increase. However, the effects of impurities and their catalytic action can easily override the density effects. Purified data shows the density difference more clearly, but it is, nevertheless, relatively small when other factors are considered.

Oxidation Threshold
Purified Graphite Grades
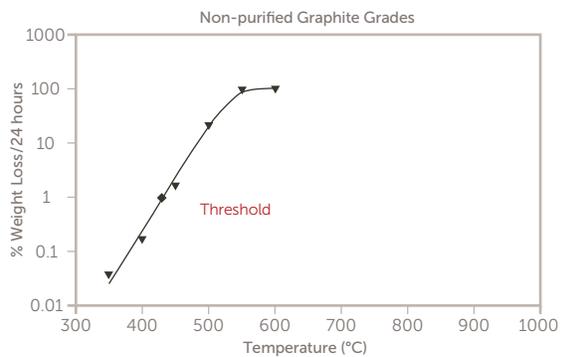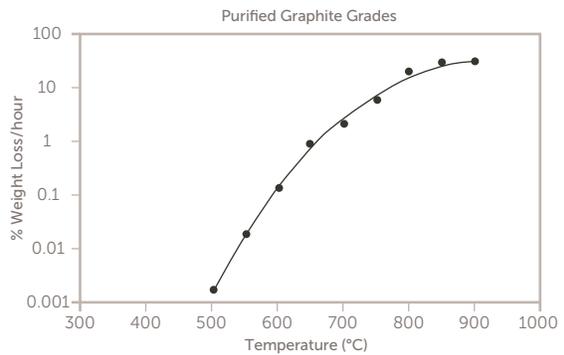

Oxidation Threshold
Non-purified Graphite Grades
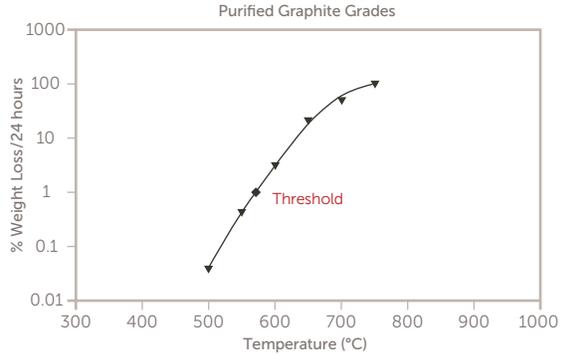
Figure 18-1. Oxidation threshold

Oxidation Rate
Purified Graphite Grades

Oxidation Rate
Non-purified Graphite Grades
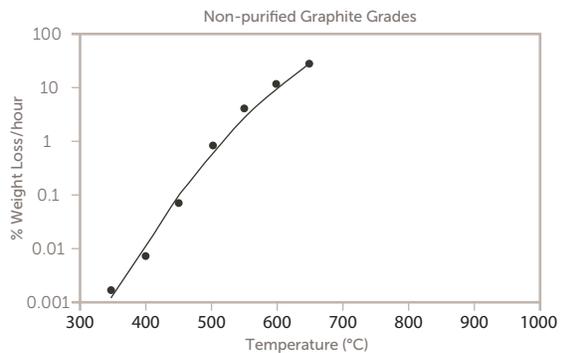
Figure 18-2. Oxidation rate

APPENDIX A

Prefix conversion factors

Prefix	Symbol	Unit multiplier
Giga	G	10^9
Mega	M	10^6
Kilo	K	10^3
Deci	d	10^{-1}
Centi	c	10^{-2}
Milli	m	10^{-3}
Micro	µ	10^{-6}
Nano	n	10^{-9}
Pico	p	10^{-12}

Density conversion factors

From	To	Multiply by
g/cm^3	lb/in^3	0.03613
g/cm^3	lb/ft^3	62.428
g/cm^3	kg/m^3	1000
g/cm^3	g/m^3	1,000,000
lb/in^3	g/m^3	27,679,904.710
lb/in^3	kg/m^3	27,679.905
lb/in^3	g/cm^3	27.6799

Length conversion factors

From	To	Multiply by
Inch	ft	0.0833
Inch	m	0.0254
Inch	cm	2.54
Inch	mm	25.4
Feet	in	12.0
Feet	m	0.3048
Feet	cm	30.48
Feet	mm	304.8
Centimeter	m	0.01
Centimeter	mm	10.0
Centimeter	µ	1.0×10^4
Microns (µ)	cm	1.0×10^{-4}
Microns (µ)	in	3.937×10^{-5}
Microns (µ)	ft	3.281×10^{-6}
Microns (µ)	m	1.0×10^{-6}
Microns (µ)	Å	1.0×10^4
Angstroms (Å)	m	1.0×10^{-10}

Strength conversion factors (pressure)

From	To	Multiply by
lb/in^2 (= psi)	lb/ft^2	144.0
lb/in^2 (= psi)	g/cm^2	70.307
lb/in^2 (= psi)	kg/cm^2	0.0703
lb/in^2 (= psi)	kg/m^2	703.07
lb/ft^2	lb/in^2	6.94×10^{-3}
lb/ft^2	g/cm^2	0.4882
lb/ft^2	kg/m^2	4.8824
kg/m^2	lb/ft^2	0.2048
kg/m^2	lb/in^2	1.422×10^{-3}
kg/m^2	g/cm^2	0.10
kg/cm^2	lb/in^2	14.223
g/cm^2	kg/m^2	10.0
g/cm^2	lb/in^2	0.01422
N/mm^2 (= MPa)	lb/in^2 (= psi)	145.032
N/mm^2 (= MPa)	kg/m^2	101.972×10^3
MN/m^2	MPa	1
N/m^2	lb/in^2 (= psi)	1.45×10^{-4}

Electrical resistivity conversion factors

From	To	Multiply by
Ω•in	Ω•cm	2.54
Ω•in	Ω•m	0.0254
Ω•in	Ω•ft	0.3333
μΩ•in	Ω•in	1.0×10^6
Ω•ft	Ω•in	12.0
Ω•ft	Ω•cm	30.48
Ω•ft	Ω•m	0.3048
Ω•cm	Ω•in	0.3937
Ω•cm	μΩ•in	393.7×10^3
Ω•cm	Ω•ft	0.0328
Ω•cm	Ω•m	0.01
Ω•m	Ω•in	39.37
Ω•m	Ω•ft	3.281
Ω•m	Ω•cm	100.0
Ωmm²/m	Ω•m	1.0×10^{-6}
Ωmm²/m	Ω•cm	1.0×10^{-4}

Coefficient of thermal expansion

From	To	Multiply by
(in/in)/°C	(in/in)/°F	0.5556
1/°C	1/°F	0.5556
(in/in)/°F	(in/in)/°C	1.80
1/°F	1/°C	1.80

Conversion constants for 1/°C to 1/°F and 1/°F to 1/°C are true for any dimensional unity, i.e., in/in, cm/cm, ft/ft, m/m.

Thermal conductivity conversion factors

From	To	Multiply by
(BTU•ft/hr/ft² °F)	(cal cm)/(cm² sec °C)	4.134×10^{-3}
(BTU•ft/hr/ft² °F)	(Kcal cm)/(m² hr °C)	148.8
(BTU•ft/hr/ft² °F)	(kilowatt hr in)/(ft hr °F)	3.518×10^{-3}
(BTU•ft/hr/ft² °F)	(kilowatt hr in)/(ft hr °F)	12.00
(BTU•ft/hr/ft² °F)	(BTU•in/ft²/sec °F)	3.33×10^{-3}
(BTU•ft/hr/ft² °F)	(watts cm)/(cm² °C)	0.0173
(BTU•ft/hr/ft² °F)	(cal cm)/(cm² hr °C)	14.88
(BTU•ft/hr/ft² °F)	(BTU•in/ft²/day °F)	288.0
(BTU•ft/hr/ft² °F)	W/m•K	0.0173
1 calorie = 1 cal = 1 gram cal		
1 calorie = 1 kilogram cal = 1 Kcal = 1000 cal		

APPENDIX B

Research & development laboratory instructions

Number	Instruction
4.1.1.1	Apparent Density of Carbon and Graphite Articles
4.1.1.2	Electrical Resistivity of Carbon and Graphite
4.1.1.3	Shore Scleroscope Hardness of Carbon and Graphite
4.1.1.4	Rockwell Hardness of Graphite
4.1.1.5	Coefficient of Thermal Expansion (CTE) of Graphite
4.1.1.6	Ash Analysis
4.1.1.7	Oxidation Resistance Test Method
4.1.1.8	Oxidation Threshold Test Method
4.1.1.13	Flexural Strength of Carbon and Graphite
4.1.1.14	Compressive Strength of Carbon and Graphite
4.1.1.15	Polishing Samples for Photomicrographs
4.1.1.16	Microphotography and Examination of Carbon and Graphite
4.1.1.19	Permeability of Graphite Plates
4.1.1.22	Equotip Hardness of Carbon and Graphite

APPENDIX C BIBLIOGRAPHY

"Anodes of the Aluminium Industry," R&D Carbon Ltd., P.O. Box 157, CH-3960, Sierre, Switzerland.

Brixius, W.H., Dagdigian, J.V., "Mercury Porosimetry Analysis of Fine-Grained Graphite," Conf. Proc., 16th Biennial Conference on Carbon, (1983), pp. 465–466.

Brooks, J.D. and Taylor, G.H., "The Formation of Some Graphitizing Carbons," Chemistry and Physics of Carbon, Ed. Walker, P.L., Jr., Dekker, M., New York, 4, 243–283 (1968).

Bundy, F.P., Bassett, W.A., Weathers, M.S., Hemley, R.J., Mao, H.K. and Goncharov, A.F., The Pressure- Temperature Phase and Transformation Diagram for Carbon; Updated Through 1994, Carbon, 34, 141–153, (1996).

Campbell, I.E. and Sherwood, E.M., High Temperature Materials and Technology, New York: John Wiley & Sons, Inc., 1967.

Cezairliyan, A. and Righini, F., "Measurements of Heat Capacity, Electrical Resistivity, and Hemispherical Total Emittance of Two Grades of Graphite in the Range of 1500° to 3000°K by a Pulse Heating Technique," Rev. in. Htes Temp. et Refract. t.12 (1975), pp. 124–131.

Fitzer, E., Köchling, K.-H., Boehm, H.P. and Marsh, H., "Recommended Terminology for the Description of Carbon as a Solid," Pure and Applied Chemistry, 67, 473–506 (1995).

Grenis, A.F. and Levitt, A.P., The Spectral Emissivity and Total Normal Emissivity of Graphite at Elevated Temperatures. (Watertown, Mass.: Watertown Arsenal Laboratories, November, 1959. [NTIS No. ADA951659]).

Hasselman, D.P.H., Becher, P.F., Mazdiyasni, K.S., "Analysis of the Resistance of High-E, Low-E Brittle Composites to Failure by Thermal Shock," Z. Werkstofftech. 11 (1980), 82–92.

Heintz, E.A., "The Characterization of Petroleum Cokes," Carbon, 34, 699–709 (1996).

The Industrial Graphite Engineering Handbook, New York: Union Carbide Corporation, 1969.

Kelly, B.T., Physics of Graphite, London: Applied Science Publishers Ltd, 1981.

Kennedy, A.J., Graphite as a Structural Material in Conditions of High Thermal Flux. (Cranfield: The College of Aeronautics, November 1959. [CoA Report No. 121]).

King, C.R., "Development of an Experimental Technique to Thermally Shock Graphites," Carbon, 8 (1970), 479–484.

Kingery, W.D., Introduction to Ceramics, New York: John Wiley & Sons, Inc., 1960.

Kingery, W.D., Journal of the American Ceramic Society, 38 (1955).

Liu, Y., Xue, J.S., Zheng, T. and Dahn, J.R., "Mechanism of Lithium Insertion in Hard Carbons Prepared by Pyrolysis of Epoxy Resins," Carbon, 34, 193–200 (1996).

Lockyer, G.E., Lenoe, E.M., Schultz, A.W., Investigation of Nondestructive Methods for the Evaluation of Graphite Materials. (Lowell, Mass.: AVCO Corporation, September 1966. [AFML-TR-66-101]).

Loison, R., Foch, P. and Boyer, A., "Coke: Quality and Production," Butterworths, London (1989).

Marsh, H. et al., Introduction to Carbon Technologies, (1997), pp. 4, 521.

Marsh, H. and Diez, M.A. "Liquid Crystalline and Mesomorphic Polymers," Eds. V.P. Shibaev and L. Lam, Ch. 7, Mesophase of Graphitizable Carbons, Springer- Verlag, New York, 231–257 (1994).

"Materials Selector 1987," Materials Engineering, Cleveland, Ohio: Penton Publishing, December 1986.

Matsumura, Y., Wang, S. and Mondori, J., "Interactions between Disordered Carbon and Lithium Ion Rechargeable Batteries," Carbon, 33, 1457–1462 (1995).

Orr, C., Jr., "Application of Mercury Penetration to Materials Analysis," Publication 9-AN-1 from Micromeritics Instrument Corporation, 8.

Petroski, H., "The Pencil – A History of Design and Circumstance," Alfred A. Knopf, New York (1990).

Reynolds, W.N., Physical Properties of Graphite, Amsterdam: Elsevier Publishing Co. LTD., 1968.

Rossi, R.C., "Thermal-Shock Resistant Materials," Materials Science Research, 5 (1971), 12–136.

Sato, S., Hwaji, H., Kawamata, K. and Kon, J., "Resistance and Fracture Toughness Against Thermal Shock of Several Varieties of Graphite," The 22nd Japan Congress on Materials Research – Metallic Materials, Mito, Japan: March 1979.

Sato, S., Sato, K., Imamura, Y. and Kon, J., Carbon, 13 (1975).

Serlie, M. and Oye, H.A., "Cathodes in Aluminium Electrolysis," 2nd Edition, Dusseldorf, Germany, Aluminium-Verlag (1994).

Spain, I.L., Electronic Transport Properties of Graphite, Carbons, and Related Materials, Chemistry and Physics of Carbon, 16 (1981), p. 119.

Taylor, R.E. and Groot, H., Thermophysical Properties of POCO Graphite. (West Lafayette, Indiana: Purdue University, July 1978. [NTIS No. ADA060419]).

Walker, P.L., Jr., Chemistry and Physics of Carbon, New York: Marcel Dekker, Inc., Vols.1–7, 1965–1971.

Walker, P.L., Jr. and Thrower, P.A., Chemistry and Physics of Carbon, New York: Marcel Dekker, Inc., Vols. 8–17, 1973–1981.

Washburn, E.W., Phys. Rev., 17, 273 (1921).

Wirt, W., "Specific Heat of POCO Graphite AXF-5Q at Several Temperatures Between 30–500°C," Job No. 84-826 Prepared for Maxwell Laboratories, Analytical Service Center, September 18, 1984.

Xue, J.S. and Dahn, J.R., "Dramatic Effect of Oxidation on Lithium Insertion in Carbons Made from Epoxy Resins," J. Electrochem. Soc., 142, 3668–3677 (1995).

Zhao, J., Wood, J.L., Bradt, A.C. and Walker, P.L., Jr., "Oxidation Effects on CTE and Thermal Shock Fracture Initiation in Polycrystalline Graphites," Carbon, 19 No. 6, (1981), 405–408.

References

[1] Adapted from Marsh, H. et al., Introduction to Carbon Technologies, (1997), pp. 4, 521.

[2] Spain, I.L., Electronic Transport Properties of Graphite, Carbons, and Related Materials, Chemistry and Physics of Carbon, 16 (1981), p. 119.

[3] See footnote 1.

[4] Brixius, W.H., Dagdigian, J.V., "Mercury Porosimetry Analysis of Fine- Grained Graphite," Conf. Proc., 16th Biennial Conference on Carbon, (1983), pp. 465–466.

[5] Washburn, E.W., Phys. Rev., 17, 273 (1921).

[6] Orr, C., Jr., "Application of Mercury Penetration to Materials Analysis," Publication 9-AN-1 from Micromeritics Instrument Corporation, 8.

[7] Taylor, R.E. and Groot, H., Thermophysical Properties of POCO Graphite. (West Lafayette, Indiana: Purdue University, July 1978. [NTIS No. ADA060419]), p.16.

[8] Kingery, W.D., Journal of the American Ceramic Society, 38 (1955), p. 3.

[9] Sato, S., Sato, K., Imamura, Y. and Kon, J., Carbon, 13 (1975), p. 309.

[10] Kennedy, A.J., Graphite as a Structural Material in Conditions of High Thermal Flux. (Cranfield: The College of Aeronautics, November 1959. [CoA Report No. 121]), p.15.

[11] Sato, S., Hwaji, H., Kawamata, K. and Kon, J., "Resistance and Fracture Toughness Against Thermal Shock of Several Varieties of Graphite," The 22nd Japan Congress on Materials Research – Metallic Materials, Mito, Japan: March 1979, 67-68.

[12] Taylor, R.E. and Groot, H., Thermophysical Properties of POCO Graphite. (West Lafayette, Indiana: Purdue University, July 1978. [NTIS No. ADA060419]), p.15.

[13] Grenis, A.F. and Levitt, A.P., The Spectral Emissivity and Total Normal Emissivity of Graphite at Elevated Temperatures. (Watertown, Mass.: Watertown Arsenal Laboratories, November 1959. [NTIS No. ADA951659]), p.14.

[14] Cezairliyan, A. and Righini, F., "Measurements of Heat Capacity, Electrical Resistivity, and Hemispherical Total Emittance of Two Grades of Graphite in the Range of 1500 to 3000 K by a Pulse Heating Technique," Rev. in Htes Temp. et Refract., t.12 (1975), p. 128.

FOR MORE INFORMATION

Please call our Customer Service Center today to learn what our premium graphite and silicon carbide solutions can do for you. Visit poco.entegris.com/contact-us for the location nearest you.

TERMS AND CONDITIONS OF SALE

All purchases are subject to Poco Graphite's Terms and Conditions of Sale. To view and print this information, visit poco.entegris.com/terms-and-conditions.